THESIS FOR THE DEGREE OF DOCTOR OF PHILOSOPHY

Solid Fuel Conversion in Dual Fluidized Bed Gasification − Modelling and Experiments

LOUISE LUNDBERG

Department of Space, Earth and Environment

CHALMERS UNIVERSITY OF TECHNOLOGY

Göteborg, Sweden 2018

Solid Fuel Conversion in Dual Fluidized Bed Gasification – Modelling and Experiments
LOUISE LUNDBERG
ISBN 978-91-7597-788-1

Doktorsavhandlingar vid Chalmers tekniska högskola
Ny serie nr 4469
ISSN 0346-718X

Department of Space, Earth and Environment
Chalmers University of Technology
SE–412 96 Göteborg
Sweden
Telephone + 46 (0)31–772 1000

Printed by Chalmers Reproservice
Göteborg, Sweden 2018

Solid Fuel Conversion in Dual Fluidized Bed Gasification − Modelling and Experiments

LOUISE LUNDBERG
Division of Energy Technology
Department of Space, Earth and Environment
Chalmers University of Technology

Abstract

Dual fluidized bed gasification (DFBG) is the initial step towards the transformation of ligno-cellulosic materials into a raw gas, which can be further upgraded into transportation fuels, such as substitute natural gas, Fischer-Tropsch diesel, dimethyl ether, and methanol. DFBG units can be operated in two distinctly different ways, depending on whether the main product is a gas (to be refined into a transportation fuel) or heat and power (with gas as a by-product). For efficient operation in either mode, the degree of char conversion in the gasification chamber needs to be controlled and optimised. For this purpose, extensive knowledge is required regarding how the degree of char gasification is affected by different parameters.

The aim of this thesis is to identify and fill key knowledge gaps regarding how different parameters influence solid fuel conversion in the gasification chamber of a DFBG unit, using a combination of laboratory-scale experiments and semi-empirical modelling. In addition, the possibility of ensuring adequate fuel conversion for either of the target modes described above is investigated.

The results of the experiments presented in this thesis confirm that the laboratory-scale conditions applied in the experimental determination of reactivity data aimed at modelling fluidized bed gasification should, as much as possible, mimic the conditions of the end-scale reactor to be modelled. In particular, the effects of fuel axial mixing and of catalytic bed materials on char gasification were found to be significant.

A validated semi-empirical 1D model of the gasification chamber of a DFBG unit has been formulated that: 1) accounts for the effect of fuel axial mixing on the char gasification rate; and 2) introduces a computationally efficient method for describing fuel conversion in fluidized beds. The modelling results show that the dominance of fuel convection over fuel dispersion increases with scale. Satisfactory fuel conversion is easily achieved when heat and power are the main products, with gas as a by-product. However, when the main goal is to improve the efficiency of gas production, a combination of baffles, properly chosen operational conditions, and/or the use of an active bed material is likely necessary to achieve sufficient fuel conversion.

Keywords: dual fluidized bed gasification, biomass, fuel conversion, char gasification rate, char reactivity, fuel mixing, semi-empirical modelling, active bed material

List of Publications

This thesis is based on the following papers, which are referred to in the text according to their Roman numerals:

Paper I Lundberg, L., Johansson, R., Pallarès, D., Thunman, H. A Conversion-class model for describing fuel conversion in large-scale fluidized bed units. *Fuel*, 2017, 197, 42–50.

Paper II Lundberg, L., Pallarès, D., Thunman, H. Upscaling effects on char conversion in dual fluidized bed gasification. *Energy & Fuels*, 2018, 32, 5933–5943.

Paper III Lundberg, L., Soria-Verdugo, A., Pallarès, D., Johansson, R., Thunman, H. The role of fuel mixing on char conversion in a fluidized bed. *Powder Technology*, 2017, 316, 677–686.

Paper IV Lundberg, L., Tchoffor, P.A., Pallarès, D., Johansson, R., Thunman, H., Davidsson, K. Influence of surrounding conditions and fuel size on the gasification rate of biomass char in a fluidized bed. *Fuel Processing Technology*, 2016, 144, 323–333.

Paper V Lundberg, L., Tchoffor, P.A., Pallarès, D., Thunman, H., Davidsson, K. Influence of bed material activation and fuel moisture content on the reactivity of biomass char in a fluidized bed gasifier. *Under preparation*.

Related papers not included in this thesis:

Lundberg, L., Pallarès, D., Johansson, R., Thunman, H. A 1-Dimensional Model of Indirect Biomass Gasification in a Dual Fluidised Bed System. 11th International Conference on Fluidized Bed Technology, CFB 2014, Chemical Industry Press, Beijing, 2014, pp. 607-612. Not included in the thesis because **Paper II** covers the contents.

Lundberg, L., Tchoffor, P.A., Johansson, R., Pallarès, D. Determination of Kinetic Parameters for the Gasification of Biomass Char Using a Bubbling Fluidised Bed Reactor. 22nd International Conference on Fluidized Bed Conversion, Turku, Finland, 2015. Not included in the thesis because **Papers IV** and **V** cover the contents.

Contributions

Louise Lundberg is the main author of **Papers I–V**. She is responsible for the modelling work in **Papers I–III** (except for the particle model in **Paper I**), and for the data evaluation and part of the experimental work in **Papers IV** and **V**.

Professor Henrik Thunman (main supervisor) contributed with ideas, concepts, discussions, and guidance, as well as with the editing of **Papers I–V**. Associate Professor David Pallarès (assistant supervisor) contributed with ideas regarding the design of the experiments and the model, discussions and guidance, and with the editing of **Papers I–V**. Dr. Robert Johansson (assistant supervisor during the first four years of the PhD studies) contributed with discussions about modelling, guidance, and with the editing of **Papers I**, **III**, and **IV**. He also supplied the particle model used in **Paper I**.

Associate Professor Antonio Soria-Verdugo conducted the experiments in **Paper III** and contributed with its editing. Dr. Placid Atongka Tchoffor assisted in the experimental work in **Paper IV**, is responsible for part of the experimental work in **Paper V** (the experiments using wood pellets and forest residue pellets, as well as the SEM-EDX and line-scanning analyses), and assisted, together with Dr. Kent Davidsson, in the editing of **Papers IV** and **V**.

Acknowledgements

I would like to start by expressing my sincere gratitude to my supervisors. Henrik, thank you for helping me see the broader perspective of things and for all your ideas and inputs on the modelling work and on writing papers. David, thank you for your help with developing the model and with the writing. I greatly appreciate all our discussions and that it is so easy to talk to you about anything. Robert, I'm really thankful for all your help with the modelling work, with writing papers and for all our discussions during the first four years of my PhD studies.

Malin, I can't imagine a better roomie than you! Thank you for all our discussions (both work-related and private) and for being such a good friend. I will miss seeing your face every morning, but I know we will always stay friends, no matter what life brings us.

Placid and Kent, thank you for welcoming me into your lab, for interesting discussions and for valuable inputs regarding the papers. Antonio, thank you for providing me with important experimental data and for your assistance in writing one of the papers.

Thanks to everyone in the gasification group, both current and previous members. A special thanks to Erik, Anton, Mikael, and Teresa for providing me with essential experimental data and helpful discussions.

Thanks to the A-team, you guys are awesome! And to everyone at Energy Technology, thank you for making our division such a nice place to work at.

I doubt I would have come this far without my family and friends. Mum and dad, thank you for all your support and for always believing in me. Karin, thank you for your advice on whether or not I should do a PhD and on what I needed to consider. It was very good advice! Lina, thank you for taking my mind off work when I needed a break. Harry, thank you for being the best kid ever and for finally sleeping really well! And Simon, thank you for your love, help, support, and for being strong when I need you the most. You're the best!

This work has been financed by the Swedish Gasification Centre (SFC) within the framework of the Centre for Indirect Gasification of Biomass (CIGB); and Energiforsk, the Swedish Energy Agency, and Göteborg Energi within the framework of the project *Koksomvandling i indirekt förgasning i fluidiserade bäddar* (39972–1).

Table of Contents

Artwork

The figures in this thesis are all original artwork/result figures by the author with the following exceptions:

Figure 2.2	Artwork taken from Larsson et al. [1], modified by the author
Figure 4.1	Original artwork by Dr. Placid Atongka Tchoffor, modified by the author
Figure 5.1b	Original artwork by Dr. Erik Sette, modified by the author
Figure 5.4	Artwork taken from Larsson et al. [1]

1. Introduction

A strong societal and political drive for the implementation of a circular economy that will be independent of fossil fuels is underway worldwide. The combustion of fossil fuels results in CO_2 emissions and is to a large part responsible for the increased levels of greenhouse gases in the atmosphere. This in turn has led to an increase in global temperature and, consequently, climate change [2]. According to the Paris agreement, the increase in global average temperature should be kept "well below 2°C above pre-industrial levels" [3].

The Government of Sweden has set the goal that the domestic transportation sector should be fossil-independent in Year 2030. Since one-third of Sweden's greenhouse gas emissions originate from the transportation sector [4], achieving this goal would result in climate benefits due to a substantial reduction in CO_2 emissions, as well as in a significant weakening of Sweden's dependence on fossil fuels.

Biomass, which is an abundant resource in several countries (e.g., Sweden), is predicted to play a role in achieving the abovementioned climate goals [5]. Biomass can be considered to be climate neutral, with several possible areas of application such as in district heating, replacing oil in plastic manufacturing, and in the production of heavy-vehicle transportation fuels [5]. Furthermore, the combination of biomass combustion and carbon capture and storage (BECCS) is put forward as an efficient way to achieve negative CO_2-emissions (i.e., decreasing the concentration of CO_2 in the atmosphere) [6].

Biomass gasification is a key technology for the transformation of lignocellulosic materials into a raw gas, which can thereafter be upgraded to transportation fuels, such as substitute natural gas (SNG), Fischer-Tropsch diesel, dimethyl ether (DME), and methanol [7, 8]. There are currently three major gasification techniques: 1) entrained-flow gasification (EFG), in which very fine fuel particles are gasified in a high-velocity flow of O_2 or in an O_2/H_2O mixture [8, 9]; 2) direct fluidized bed gasification (FBG) [8, 9], in which the fuel, bed material, and fluidizing medium (pure O_2 or a mixture of O_2 and H_2O) are introduced together into a single fluidized bed; and 3) indirect fluidized bed gasification (also known as dual fluidized bed gasification, DFBG), which consists of two fluidized bed reactors, one combustor and one gasifier [7, 9]. In EFG and FBG, the heat required to sustain the endothermic gasification reactions is supplied by burning part of the fuel, whereas in DFBG this heat is supplied by circulating the bed material between the combustor and the gasifier (Figure 1.1). Table 1.1 summarises the main characteristics of the three techniques.

Table 1.1 Operational conditions, advantages, and disadvantages associated with EFG, FBG, and DFBG [7-9].

	EFG	FBG	DFBG
O_2 production/dilution with N_2	Yes	Yes	No
Maximum temperature	>1600ºC*	800º–1000ºC	750º–1000ºC
Yields of tars and by-products	Low	High	High
Fuel grinding required	Yes	No	No
Suitable for pressurisation	Yes	Yes	No
Fuel burnout	Yes	No	Yes

*High temperatures are needed to avoid extensive soot formation [9], and to produce pure syngas that consists exclusively of CO, H_2, H_2O, and CO_2.

While EFG and FBG are mature techniques for coal gasification, with commercial-scale plants operating worldwide (see for example, [10] and [11], respectively), the up-scaling of DFBG is in progress (Table 1.2). Of the different combinations of fluidized bed types used in DFBG, the most popular is the one in which the combustor is a circulating fluidized bed (CFB) and the gasifier is a bubbling fluidized bed (BFB) [12], and it corresponds to the design of the operational state-of-the-art biomass DFBG units given in Table 1.2. Two of the units listed in Table 1.2 are considered in this thesis: the Chalmers DFBG unit [1] (see Section 5.3.1), and the GoBiGas plant [13], which is an industrial DFBG unit for transforming biomass to SNG.

Table 1.2. Operational biomass DFBG units with a CFB combustor and a BFB gasifier.

Unit	Plant type	Thermal input/product	Start-up year	Reference
GoBiGas	New design	32 MW_{th}/20 MW_{SNG}	2013	[13]
Senden	New design	14 MW_{th}/5 MW_{el}	2011	[14]
Oberwart	New design	8.5 MW_{th}/2.8 MW_{el}	2008	[15]
Güssing	New design	8 MW_{th}/2 MW_{el}	2002	[16]
Burgeis	New design	2 MW_{th}/0.5 MW_{el}	2012	[17]
Chalmers	Retrofit	2–4 MW_{th}/*	2007	[1]
IHI Tigar**	New design	6–9 MW_{th}/1800 Nm^3 syngas/day	2015	[18]

*The raw product gas is torched in the CFB boiler.

**Ready for commercialisation in 2018.

This thesis focuses on the DFBG technology using a BFB gasifier. A DFBG unit (Figure 1.1a) can be designed/operated in two distinctly different modes, depending on whether the main product is: 1) a gas, to be refined into a transportation fuel; or 2) heat and power, with gas as a by-product. The combustor in a DFBG system converts the char that remains after passage through the gasification chamber, and the thermal power in the combustor is thus given by Eq. (1.1). (All the variables, parameters, and constants that are used in the equations, figures, and tables of this thesis are described in the Notation on page 45.)

$$P_{\mathrm{comb}} = \dot{m}_{\mathrm{F}} Y_{\mathrm{char}} \left(1 - X_{\mathrm{char,g}}\right) LHV_{\mathrm{char}} = \frac{Y_{\mathrm{char}} \left(1 - X_{\mathrm{char,g}}\right) LHV_{\mathrm{char}}}{LHV_{\mathrm{F}}} P_{\mathrm{tot}} \qquad (1.1)$$

If the target is gas production, the optimum overall efficiency of the system occurs when a thermal balance is achieved between the combustor [P_{comb} in Eq. (1.1)] and the internal heat demand of the DFBG unit (i.e., there is no additional fuel input to the combustor; see Figure 1.1a). This occurs when the degree of char conversion in the gasification chamber, $X_{\mathrm{char,g}}$ in Eq. (1.1), is at its optimal value, $X_{\mathrm{char,g}}^{\mathrm{opt}}$. Below this value cooling must be supplied, and above this value a part of the raw gas needs to be combusted (see Figure 1.1b). The value of $X_{\mathrm{char,g}}^{\mathrm{opt}}$, which typically lies in the range of 10%–50% [1], depends on the applied biomass fuel, the desired end-product, and the flows and temperatures of the inputs to the gasifier. For SNG production, the degree of char gasification should be slightly above the optimal value, so as to ensure that additional cooling is not needed, without burning excessive amounts of the raw gas. However, for certain end-products (e.g., Fischer-Tropsch diesel), it is desirable to gasify as much char as possible to obtain a raw gas with high concentrations of CO and H_2. Thus, $X_{\mathrm{char,g}}^{\mathrm{opt}}$ can be regarded as the minimum acceptable degree of char gasification.

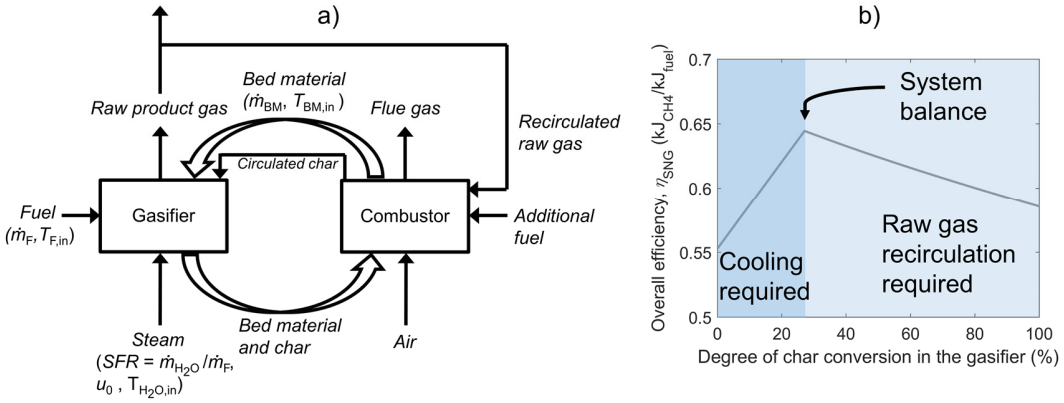

Figure 1.1. a) Principle of DFBG. b) Overall efficiency as a function of the degree of char gasification, exemplified for a case with SNG as the end-product.

In contrast, if gas is a by-product of heat and power production, the produced gas is derived from pyrolysis of the fuel, and the degree of char conversion within the gasification chamber should be minimised, so as to avoid an increased heat demand in the gasifier. Furthermore, designing a DFBG plant such that its operation can be switched between these two modes (a so-called 'poly-generation unit') would increase the flexibility of the DFBG technology, which is proposed as a critical component of thermochemical fuel conversion units in an energy system that has an increased share of non-dispatchable heat and power.

As the time-scale for pyrolysis is much shorter than that for char gasification, it is necessary to provide sufficient heat to convert the volatiles, as well as a fuel residence time that allows sufficient char conversion. For efficient operation of either of the two aforementioned modes, it is desirable to be able to control and optimise the degree of char conversion in the gasification chamber. For

this purpose, improved knowledge of how different parameters affect the degree of char gasification is required (Figure 1.3).

1.1. Aim and Scope

The aim of this thesis is to identify and fill key knowledge gaps regarding how different parameters influence solid fuel conversion in the gasification chamber of a DFBG unit. Parameters that affect the fuel residence time (e.g., fuel mixing) and the char gasification rate (e.g., active bed materials) are considered.

Furthermore, the possibility of ensuring sufficient fuel conversion for either of the two target modes (exclusively gas production or heat and power production with gas as a by-product) is investigated. The acquired knowledge is then applied to formulate methods that can be used in the design, up-scaling, retrofitting, and control/optimisation of DFBG units.

The scope of the thesis (and thus, the conclusions drawn from the modelling results) is limited to DFBG units with a BFB gasifier that has a rectangular geometry. The model includes the bottom bed of a BFB gasifier, discretised in one lateral direction (that of the solids cross-flow).

1.2. Methodology

A combination of semi-empirical modelling (see Section 2.3) and laboratory-scale experiments on targeted phenomena was applied in this thesis. Figure 1.2 shows the methodology employed. In brief, the model, which is described and validated in **Papers I–III**, in Chapter 5, and in Section 6.2.2, has been developed and refined over time. After identifying critical knowledge gaps (see Chapter 2), laboratory-scale experiments were conducted (see **Papers IV** and **V**, Chapter 4, and Section 6.1) and the results from these experiments were then used to improve the model. Once the model simulations agreed sufficiently well with measurements from the Chalmers gasifier (see Section 5.3.1), the model was used to investigate the effects of different factors, such as operational conditions and gasifier scale, on the fuel conversion.

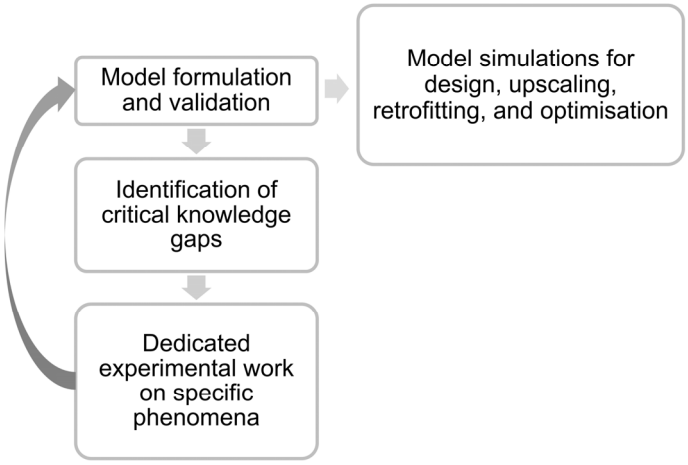

Figure 1.2. Methodology applied in this thesis.

1.3. Thesis Outline

Figure 1.3 shows how the papers included in the thesis are linked to the aim of increasing the knowledge of how different parameters affect the fuel conversion in DFBG. It should be noted that only the factors considered in the papers of this thesis are included in Figure 1.3 (volatiles inhibition, for instance, which affects the char gasification rate [19], is not included). A brief description of each paper is given in Table 1.3.

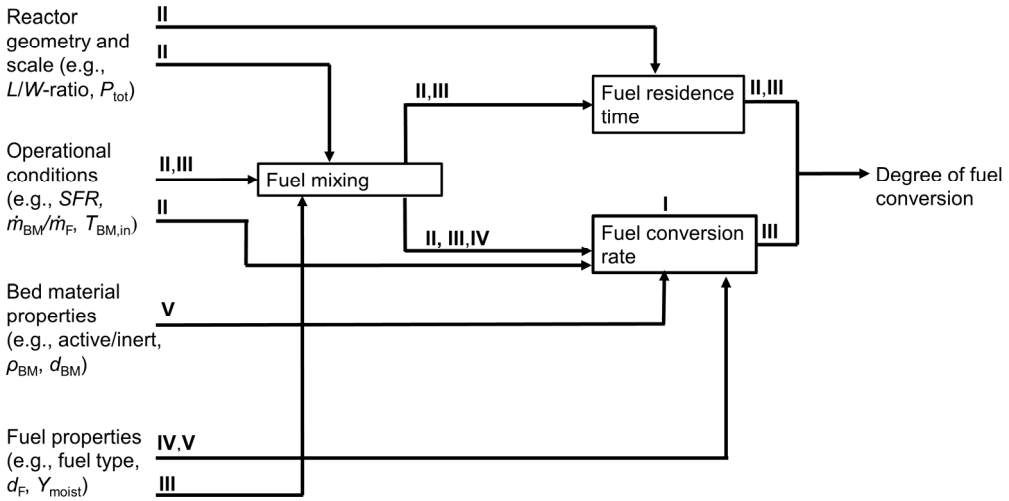

*Figure 1.3. Flow chart showing the influences of the investigated parameters on the degree of fuel conversion. The Roman numerals **I–V** indicate the papers related to the topics of the thesis.*

Table 1.3. Description of the papers included in the thesis.

Paper	Description
I	A computationally efficient method for describing fuel conversion in fluidized beds using population balances is developed and verified.
II	The effects of unit scale on the process performance and optimisation are investigated. Methods for achieving sufficient fuel conversion in large-scale DFBG units are proposed.
III	The effects of lateral vs. axial mixing of the fuel on char conversion in the gasification chamber of a DFBG unit, as well as the effects of operational conditions on the dominant mixing mechanisms, are determined.
IV	The impacts on the char gasification rate of fuel axial mixing, fuel concentration, pyrolysis atmosphere, fuel structure (i.e., crushed or intact pellets), and cooling of the char after pyrolysis are investigated and quantified.
V	The influences of the bed material and the fuel moisture content on the char reactivity in a fluidized bed are investigated for wood chips of different sizes. Furthermore, the specific effect of bed material activation on the char gasification rate is investigated and quantified.

2. Background

2.1. Parameters Affecting the Fuel Conversion

As shown in Figure 1.3, the degree of fuel conversion within the gasification chamber of a DFBG unit depends on the fuel residence time and the fuel conversion rate, both of which are in turn dependent upon other factors, such as the fuel mixing, reactor geometry and scale, operational conditions, and the bed material and fuel properties.

The fuel residence time (see Chapter 3), increases with reactor size and decreases with fuel lateral mixing (which increases with an increase in fluidization velocity and/or solids cross-flow [20] and is enhanced if the fuel particles are located on the bed surface [21]). Furthermore, baffles can be used to increase the fuel residence time [9], facilitating a more compact design of the gasifier, and thereby yielding lower operational and capital costs.

The influence of operational parameters on fuel conversion through their effect on the fuel residence time is investigated in **Papers II** and **III**. Furthermore, the impacts of gasifier scale and the incorporation of baffles into the gasification chamber on the fuel residence time are considered in **Paper II**.

A biomass particle goes through three fuel conversion stages in a gasifier: 1) drying, during which the moisture in the fuel is evaporated; 2) pyrolysis, during which volatile gases exit the fuel particle; and 3) char gasification, where the C in the char reacts with H_2O (and/or CO_2 if present) to form H_2 and CO. While drying and pyrolysis depend solely on heat transfer to the fuel particle, char gasification is a more complex process. As shown in Figure 2.1, the obtained char gasification rate is a combination of the char reactivity and mass transfer limitations.

Reactivity studies on biomass char are often conducted with thermogravimetric analysis (TGA), using small fuel particles and relatively low heating rates [22, 23]. However, the process conditions, such as the heating rate (which for fluidized beds is in the range of 100º–1000ºC/s [24]) and the choice of bed material, can have significant effects on the char reactivity (see below). In line with this, previous studies have shown that to obtain data from laboratory-scale units that are useful for the modelling of industrial-scale processes, chemical similarity (i.e., that the conditions in the laboratory-scale reactor, such as the fuel particle temperature and the pressure inside the fuel particle, are similar to those in the industrial-scale unit) must apply [25].

Thus, the reactivity parameters determined using TGA are not applicable to the modelling of char gasification in a fluidized bed gasifier. Instead, to acquire relevant kinetic and structural data, a laboratory-scale fluidized bed gasifier should be employed. Fluidized bed gasifiers have previously been used to determine the reactivities of coal char (e.g., [26, 27]) and biomass char (e.g., [28, 29]).

In this thesis, the char reactivity that results from biomass gasification in a fluidized bed is designated as the "process-assisted char reactivity" (Figure 2.1), to distinguish it from the char

reactivity that results from TGA. The process-assisted char reactivity is the reaction rate in the absence of mass transfer limitations.

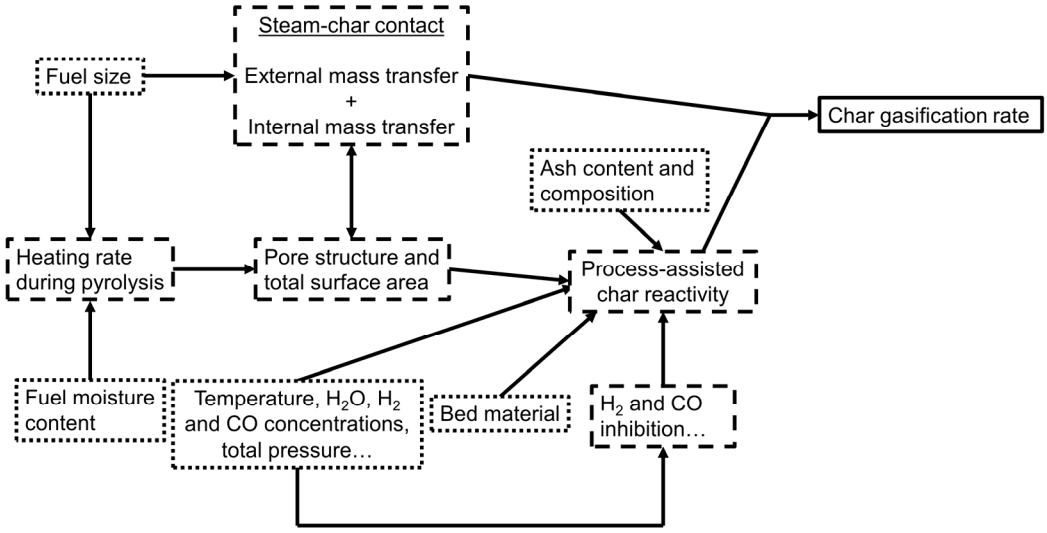

Figure 2.1. Schematic showing how the different parameters are connected to the process-assisted char reactivity and the char gasification rate. The dotted-line boxes signify inputs (fuel and bed material data/operational conditions), the dashed-line boxes are intermediates, and the solid-line box represents the output (the char gasification rate).

The size of the fuel particles affects the resistance to mass transfer. Furthermore, mass transfer becomes more dominant as the temperature increases. Nilsson et al. [24], who investigated the gasification of chars from dried sewage sludge with different sizes (1.2–3.4 mm) in a laboratory-scale fluidized bed, found that mass transfer was the limiting factor for all but the smallest particles (1.2 mm) at 900°C. In contrast, at 850°C, the observed char gasification rates were similar for all the fuel particle sizes. Thus, by choosing a sufficiently small fuel particle size for the determination of the process-assisted char reactivity, mass transfer limitations can be avoided. The effect of fuel particle size on the char gasification rate is investigated for wood pellets (crushed and intact) and for wood chips in **Papers IV** and **V**, respectively.

The char reactivity increases with temperature and steam concentration. There exists substantial variability in the reported kinetic parameters for biomass char gasification, both between different biomasses [22] and within a batch of a given biomass [30]. When TGA is used, the found variability in biomass reactivity is mainly attributed to the intrinsic heterogeneity of the ash content and composition [22]. In particular, K and Ca have been shown to catalyse char gasification [31, 32].

As mentioned above, in addition to the aforementioned intrinsic heterogeneity of biomass, several process-related parameters can affect the char reactivity, including the heating rate, the steam-char contact, and the choice of bed material (these three parameters are described in more detail below), as well as the time of pyrolysis [26, 33, 34], total pressure during char gasification [34], char cooling prior to char gasification [24], inhibitory effects of H_2 and CO [19, 28], and the gasification

atmosphere [28, 35]. In **Paper IV**, the effects of char cooling, pyrolysis atmosphere, and fuel concentration are considered for steam gasification of wood pellets.

The heating rate affects the pore structure of the char. The morphology of chars formed at low heating rates remains relatively unchanged due to the slow outflow of volatile gases [36, 37]. In contrast, the rapid outflow of volatile gases that is the consequence of a high heating rate leads to a loss of the original cellular structure of the particle, yielding a more porous char [38]. Several authors have shown that chars formed at high heating rates are 2–3-fold [22] more reactive than those produced at low heating rates [36, 39-42], and this phenomenon has been attributed to a larger total surface area and a more reactive pore structure [36, 42]. Furthermore, the recombination of C, which can occur over time, is reduced by the rapid outflow of pyrolysis gases that results from high heating rates [40].

The moisture content of the fuel affects the heating rate of the fuel particles (a wet fuel takes longer to heat than does a dry fuel), and thus possibly the resulting char structure and reactivity. The effect of moisture content on char reactivity is investigated in **Paper V** by comparing the two extremes for wood chips, i.e., a dry fuel (moisture content of 0%) and a fuel that is saturated with water (moisture content of around 40%).

The fuel size also influences the heating rate (small particles are heated faster than larger particles), and could thus potentially affect the char reactivity. However, as noted above, in the study conducted by Nilsson et al. [24], no effect of fuel size on the char gasification rate was observed at 850°C.

As indicated in Figure 2.1, in addition to influencing the resistance to mass transfer to the char particle, the steam-char contact also affects the char reactivity. This is because the total surface area and pore volume increase when the char comes into contact with steam [43, 44].

The heating rate and the steam-char contact vary depending on whether the fuel particles are present on the bed surface or within the dense bed. Thus, fuel axial mixing (which has been shown to be promoted by high fluidization velocities and low solids cross-flows [45]) can affect the char reactivity. This effect is examined in **Paper IV**. Furthermore, the effects of operational conditions on the degree of char gasification, through their influences on fuel mixing, are investigated in **Paper III**, using the results from **Paper IV**.

The choice of bed material has been shown to affect char conversion in the gasification chamber of a DFBG unit [46-49]. For example, Berdugo Vilches et al. [48] observed 6.6-fold, 3.0-fold, and 1.2-fold increases in $X_{\mathrm{char,g}}$ when switching from quartz sand to bauxite, ilmenite, and olivine, respectively. The observed effect of the bed material is explained by to the fact that some bed materials have a higher tendency than others (e.g., silica sand) to interact with the ash-species present in the fuel, such that a catalytically active ash layer is formed around the bed material particles. K, which forms gas-phase compounds such as KOH and KCl at 600°–1000°C (i.e., typical gasification temperatures) [43, 50], has been identified as being catalytically active in this process [51, 52].

In **Paper V,** the effects of bed material type on the process-assisted kinetic parameters and the shape of the conversion profile (i.e., the variation of reactivity with the degree of char gasification) are investigated by comparing the char reactivities for steam gasification of wood chips using two different bed materials: silica sand and activated olivine extracted post-operation from the GoBiGas gasifier. Furthermore, the specific effect of bed material activation on char gasification is investigated using silica sand, fresh olivine, and activated olivine as the bed materials and wood pellets and forest residue pellets as the fuels.

2.2. Up-scaling and Control of DFBG Units

In large-scale BFB units, the bed height is limited to a few decimetres because the bubble size increases with bed height, which results in a significantly decreased mass transfer of gas between the bubble and emulsion phases [53]. This in turn leads to a reduction in the steam-fuel contact, which limits char conversion.

Thus, for commercial-scale plants, cross-sectional up-scaling (i.e., increasing the cross-sectional area of the gasifier without increasing the bed height) must be applied to limit the bubble size, as well as to maintain a constant fluidization velocity. DFBG systems also offer the possibility to use high-pressure process steam to fluidize the bed, which can help to decrease the bubble size by creating a high pressure drop over the gas distributor [54], thereby improving the gas-solids mixing.

Cross-sectional up-scaling yields a larger cross-sectional area, as compared to up-scaling in all three dimensions. As a consequence, there are higher capital costs, and the circulation of bed material between the BFB gasifier with its large cross-sectional area and the comparatively small CFB combustor can create a challenge for the spatial design. Furthermore, while laboratory-scale BFB units often have a circular cross-section, for larger units, rectangular geometries would be more cost-effective because they are easier to build.

As noted in Section 2.1, the degree of char gasification in a DFBG unit is strongly dependent upon the temperature and the fuel residence time within the gasification chamber. Controlling the flow and the temperature of the solids entering the gasifier is therefore crucial for process optimisation. The temperature of the solids entering the gasifier can be controlled by installing a heat exchanger before the gasifier. Furthermore, by designing the unit such that part of the flow can bypass the gasifier, the solids flow into the gasifier can be controlled.

An example of this is the Chalmers system (see Section 5.3.1), which originally consisted of a 12-MW boiler with an external heat exchanger (termed the ‘Particle cooler’, see item 3 in Figure 2.2) connected to its return leg. It was subsequently retrofitted into a DFBG unit by adding a 2–4-MW BFB gasifier to the return leg. Thus, the circulating solids can be divided into three streams that flow: 1) through the external heat exchanger; 2) through the gasifier; and 3) directly back to the combustor.

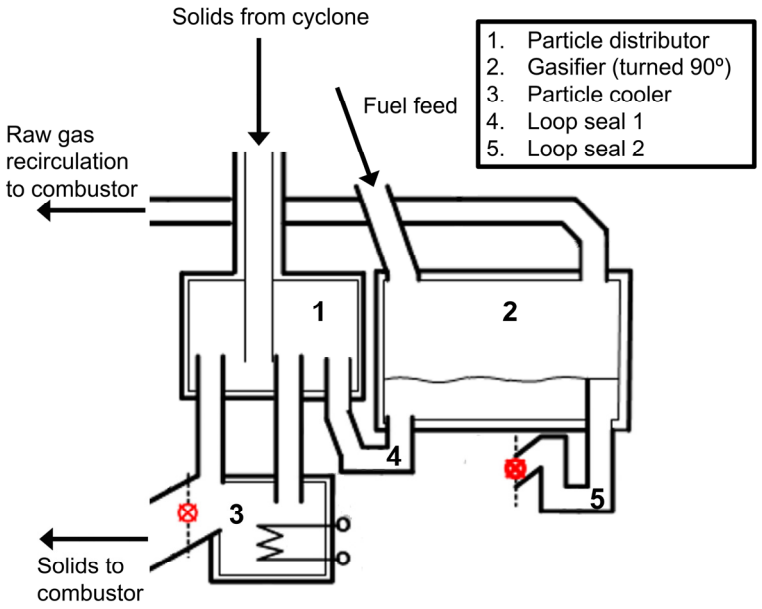

Figure 2.2. Schematic of part of the Chalmers DFBG unit, showing the particle distributor, gasifier, particle cooler, and loop seals.

2.3. Modelling of Solid Fuel Conversion in Fluidized Beds

Three major types of models are used for modelling solid fuel conversion in fluidized beds. These are (in increasing level of detail): 1) black-box (or zero-dimensional) models; 2) semi-empirical models; and 3) computational fluid dynamics (CFD) models [23]. Black-box models, in which the overall zero-dimensional heat and mass balances are solved using empirical correlations, have few inputs and are thus very simple to use, but they do not provide any information regarding the processes occurring inside the gasifier [23]. In CFD models, the velocity fields of the gas and solid components are given by solving the momentum balances, and critical assumptions need to be made regarding the interactions that occur between the different phases [23].

Semi-empirical modelling, in which the velocity fields are not given by solving the momentum transfer equations but by using simpler means, is the most widely used approach to modelling solid fuel conversion in large-scale fluidized beds (see for example, [55-58] for models of fluidized bed combustion, and [59-63] for gasification), as it offers reliability and a sufficient level of detail at a relatively low computational cost [23].

Due to the vigorous mixing in fluidized beds, fuel particles with different degrees of conversion can be, and often are, present in the same location. One way to deal with this, as is often applied in CFD models, is to track each particle (or parcel of particles) separately using Lagrangian Particle Tracking (LPT, see e.g., [64-66]). A less-accurate method, which is used mainly in zero-dimensional models but is sometimes also used for modelling drying and devolatilisation [57], is to solve one mass balance for each fuel field (moisture, volatiles, and char), while assuming a constant conversion rate for each fuel species.

A method that is more computationally affordable than LPT and that offers a higher level of detail than zero-dimensional models is the use of population balances under the assumption that fuel conversion takes place in a specific regime (e.g., the shrinking sphere regime). The fuel components (usually char) are divided into different classes based on either density or size, and one mass balance is solved for each class. In holistic modelling of CFB boilers, population balances are commonly used to model char combustion [55-58]. Population balances are used less frequently in the modelling of fluidized bed gasification, although specific cases have been reported [67].

The model presented in this thesis (for a detailed description, see **Paper II** and Chapter 5) uses semi-empirical modelling, and solid fuel conversion is described using population balances. The proposed model contains two new elements, as compared to the semi-empirical fluidized bed models found in the literature:

1) Instead of assuming a specific conversion regime and basing the classes in the population balance on either size or density, a new method is proposed. This computationally efficient method, described in **Paper I**, discretises the fuel conversion into classes based on the degree of conversion. It can be applied to different fuels with various size distributions and it is valid regardless of the fuel conversion regime.

2) The model accounts for the effect of fuel axial mixing on the char gasification rate (see Section 5.1.1). The method used for this is described in **Paper III**. In brief, it combines empirical correlations for the axial mixing of fuel during pyrolysis (from Sette et al. [45]) and char gasification (from **Paper III**) with the findings from **Paper IV** related to how the char gasification rate is influenced by fuel axial mixing.

The semi-empirical fluidized bed model used in **Papers I–III** in this thesis is based on the dimensions (width, length, and bed height) and the input data (input temperatures and mass flows, fuel and bed material properties) of the Chalmers 2–4-MW_{th} gasifier [1]. The model is validated using measurements of the degree of char conversion in the Chalmers gasifier, as taken from experiments conducted by Larsson et al. [1], Israelsson et al. [68], and Berdugo Vilches et al. [69] (see Section 5.3.1). For the scaling simulations conducted in **Paper II**, the length-to-width ratio, bed height, and superficial fuel load (in W/m^2) are the same as for the Chalmers gasifier, i.e., cross-sectional scaling is applied (see Section 2.2).

3. Theory

3.1. Fuel Residence Time

In this thesis, the average residence time of the fuel within the gasification chamber, τ_F, is estimated according to Eq. (3.1) [70]. This equation, which assumes that the velocity field of the bed material within the gasifier is uniform, combines the time-scales of the dispersive fuel flow, τ_d, [Eq. (3.2)], and the convective fuel flow induced by the cross-flow of bed material, τ_c [Eq. (3.3)].

$$\tau_F = (1/\tau_c + 1/\tau_d)^{-1} \tag{3.1}$$

$$\tau_d = L^2/(2D_F) \tag{3.2}$$

$$\tau_c = \tau_{BM}/\theta_F = m_{BM}/(\theta_F \dot{m}_{BM}) \tag{3.3}$$

The time-scale of fuel dispersion, τ_d [Eq. (3.2)], depends on the reactor length, L, and the fuel dispersion coefficient, D_F. Thus, with respect to the conditions assumed in this thesis for scaling (constant length-to-width ratio (L/W) and constant superficial fuel load in the gasifier, Q_{cr} (W/m^2), see Section 5.3), τ_d increases proportionally with the scale of the gasifier.

The time-scale of fuel convection, τ_c [Eq. (3.3)], depends on the time-scale for the mixing of the bed material within the gasifier, τ_{BM}, and the cross-flow impact factor, θ_F (see Section 5.1.1). For constant values of $\dot{m}_{BM}/\dot{m}_F$, L/W, and Q_{cr}, τ_{BM} is independent of the scale. However, since θ_F increases with the bed material velocity (see Table 5.1), which increases with scale for the geometrical assumptions made in this thesis regarding scaling, τ_c decreases with an increase in gasifier size. Thus, as the gasifier size increases, fuel convection becomes more dominant compared to fuel dispersion, i.e., the solids circulation assumes a more prominent role in the fuel residence time than does the fluidization velocity or the dense bed height.

Setting τ_d equal to τ_c and plotting D_F as a function of ($\theta_F \dot{m}_{BM}$) [Eq. (3.4)] yields a straight line, which is the boundary between the dispersion-dominant regime and the convection-dominant regime (see Figure 6.9b). Thus, Eq. (3.4) can be used to determine the dominant mixing regime for a given set of operational conditions and reactor geometry. Above this boundary [i.e., $D_F >> L^2/(2m_{BM})\cdot(\theta_F \dot{m}_{BM})$], τ_F is dominated by fuel dispersion as fuel dispersion is faster than fuel convection. Below this boundary [i.e., $D_F << L^2/(2m_{BM})\cdot(\theta_F \dot{m}_{BM})$], fuel convection is faster than fuel dispersion and thus becomes the dominant factor for τ_F.

$$D_F = L^2/(2m_{BM}) \cdot (\theta_F \dot{m}_{BM}) \tag{3.4}$$

In Section 6.2.2, Eq. (3.4) is used to determine the dominant mixing regimes within the Chalmers gasifier for a range of operational conditions. Furthermore, in Section 6.2.3, the effect of scale on the degree of char gasification, caused by its influence on the dominant mixing regimes, is investigated based on the above-described assumptions and definitions of τ_F, τ_d, and τ_c.

3.2. Char Gasification Rate and Reactivity

The degree of char gasification, $X_{\mathrm{char,g}}$, is defined as:

$$X_{\mathrm{char,g}}(t) = \frac{m_{\mathrm{C,0}} - m_{\mathrm{C}}(t)}{m_{\mathrm{C,0}}} \tag{3.5}$$

In this thesis, a clear distinction is made between the char gasification rate, R_{g}, which includes mass transfer limitations (resistance to external mass transfer to the fuel particle and pore diffusion within the particle) if such are present, and the process-assisted char reactivity, R_{pa}, for which it is assumed that there are no such limitations.

As mentioned in Section 2.1, in a study of char reactivity in a fluidized bed conducted by Nilsson et al. [24], even for the largest fuel particles used (3.2 mm), no mass transfer limitations were detected at 850°C. Furthermore, for the 'small' wood chips (thicknesses of 2–4 mm) used in the reactivity study of this thesis, the Damköhler number (which compares the reaction rate to the external mass transfer rate) and the Thiele modulus (which compares the reaction rate to the internal mass transfer rate) are estimated to be in the order of 10^{-5} and 10^{-3}, respectively for $T = 850$°C. As both factors are << 1, in the estimation of the kinetic parameters reported in Section 6.1, it is reasonable to assume that for the small wood chips there are no mass transfer restrictions at $T \leq 850$°C. Therefore, for these conditions $R_{\mathrm{g}} = R_{\mathrm{pa}}$.

In the present work, R_{g} and R_{pa} are defined using the conversion rate (i.e., normalising with the initial carbon mass of the char particle) according to:

$$R_{\mathrm{g/pa}} = \frac{dX_{\mathrm{char,g}}(t)}{dt} = \frac{\dot{m}_{\mathrm{C}}(t)}{m_{\mathrm{C,0}}} = \frac{\dot{m}_{\mathrm{C}}(t)}{m_{\mathrm{F,0}} Y_{\mathrm{char}} Y_{\mathrm{C,char}}} \tag{3.6}$$

For simplicity, n^{th}-order kinetics are chosen for the comparative study of how bed material activation can affect the process-assisted char reactivity. R_{pa} can then be expressed according to [71]:

$$R_{\mathrm{pa}} = R\left(T, p_{\mathrm{H_2O}}\right) f\left(X_{\mathrm{char,g}}\right) = k_0 e^{\frac{-E_{\mathrm{a}}}{RT}} p_{\mathrm{H_2O}}^{n} f\left(X_{\mathrm{char,g}}\right) \tag{3.7}$$

In Eq. (3.7), the last term, $f(X_{\mathrm{char,g}})$ is a structural model that accounts for structural changes within the char matrix as char conversion proceeds. Both purely empirical models (see for example, [24]) and models that attempt to describe changes in the porous structure of the char (such as the random pore model [16]) are available in the literature. In this thesis, only a qualitative analysis of $f(X_{\mathrm{char,g}})$ is conducted. The analysis focuses on $X_{\mathrm{char,g}} \approx 5\%–80\%$, which is a relevant range for DFBG. Within this range, changes in the shape of the conversion profile are relatively slow, as compared to during the start and end phases of char gasification.

4. Experiments Conducted within this Thesis

The laboratory-scale experiments conducted within the work of this thesis complement the experimental data obtained from industrial-scale units (i.e., the Chalmers gasifier and the GoBiGas unit). The experiments were carried out to investigate specific phenomena, whose effects are easier to distinguish at the laboratory scale.

The effects of the following parameters on char gasification were investigated in the experimental study conducted in this thesis: fuel axial mixing, fuel type, fuel size, fuel structure (i.e., crushed or intact pellets), fuel moisture content, fuel concentration, pyrolysis atmosphere, cooling of the char after pyrolysis, bed material type, and bed material activation (olivine).

The experimental set-up (see Figure 4.1) is described in detail in **Papers IV** and **V**. In brief, it consists of a bubbling fluidized bed reactor (7 cm i.d.) that is surrounded by an oven. The bed is fluidized with pure N_2 during pyrolysis, a mixture of N_2 and H_2O during char gasification, and air during combustion. Fuel is either added batch-wise at the top of the reactor or by placing it in a lidded wire-mesh basket that is subsequently inserted into the bed. After the gas has passed through a particle filter and a condenser, the concentrations of O_2, CO_2 and CO are logged.

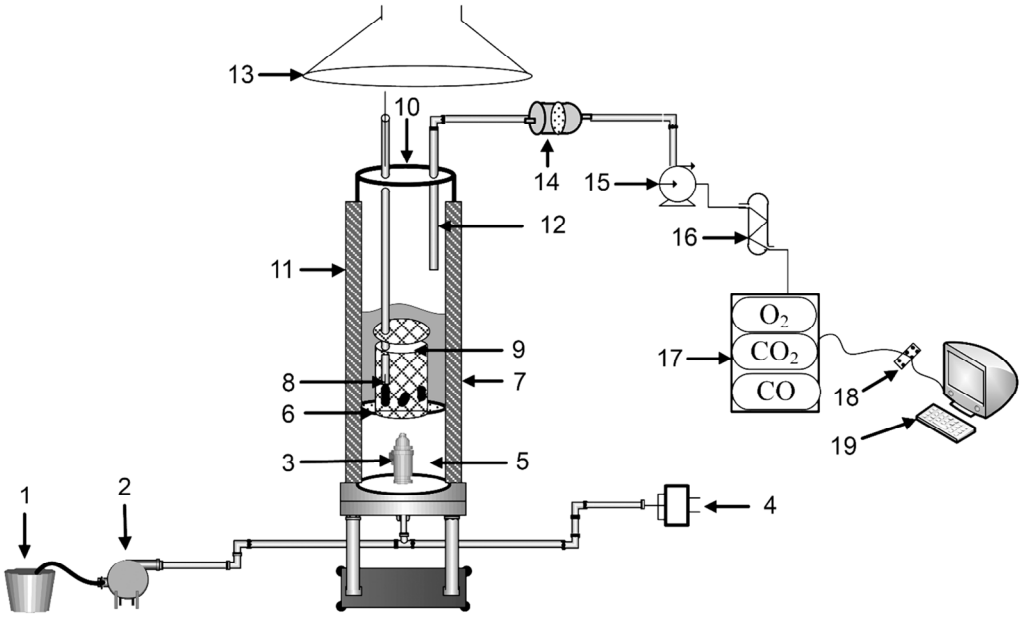

1–water tank, 2–water pump, 3–inbuilt steam generator, 4–mass-flow regulator, 5–gas preheater, 6–perforated ceramic plate, 7–bed, 8–thermocouple inserted into pellet, 9–wire-mesh basket, 10–fuel inlet when basket is not used, 11–heating elements, 12–gas probe, 13–exhaust hood, 14–particle filter, 15–gas pump, 16–condenser, 17–gas analysers, 18–PC logger, 19–computer

Figure 4.1. Experimental set-up.

In **Paper IV** (and in Section 6.1), the effect of fuel axial mixing on the char gasification rate is investigated using wood pellets as the fuel and silica sand as the bed material. The fuel particles are placed in the basket, the position of which can be adjusted so that the fuel particles are either inside the dense bed (IB) or on the bed surface (BS). Furthermore, the position of the basket can be adjusted after pyrolysis such that pyrolysis and char gasification can occur at different axial positions.

Paper V (and Section 6.1) investigates the effect of bed material activation on the char gasification rate (T = 870°C, p_{H_2O} = 0.72 bar) and the process-assisted reactivity (T = 750°–900°C, p_{H_2O} = 0.10–0.50 bar). Three bed materials (silica sand, fresh olivine, and activated olivine taken from the GoBiGas unit) and three fuels (wood chips, wood pellets, and forest residue pellets) are considered. For the wood chips, three different fuel sizes (thicknesses in the range of 2–9 mm) are employed. Furthermore, the effect of fuel moisture content on the char gasification rate is investigated by comparing the two extremes for wood chips: a dry fuel (i.e., 0% moisture) and a fuel that is saturated with water (i.e., ≈ 40% moisture).

5. Modelling

The model of the gasifier and the method used to discretise the fuel conversion are presented in Sections 5.1 and 5.2, respectively, whereas the modelled cases are described in Section 5.3. The most important assumptions made in the modelling work and their potential implications for the results are discussed in Section 6.3.2.

5.1. Model of the Gasifier

In the steady-state, semi-empirical 1D model used in this thesis (see [72] for a previous version), the dense bottom bed of the gasification chamber is discretised in the direction of the solids cross-flow. The model input/output scheme is depicted in Figure 5.1a, while Figure 5.1b shows the mass flows considered by the model, as well as the direction of discretisation. The solids are assumed to leave the gasification chamber by falling over the edge at the outlet.

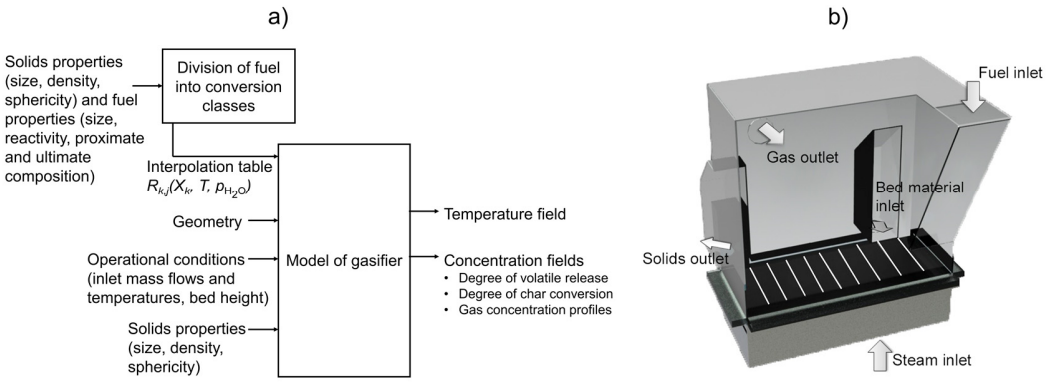

Figure 5.1 a) Model structure, and b) energy and mass flows considered by the model of the gasifier, as well as the direction of discretisation (white lines).

The model solves the mass and heat balances given by Eqs. (5.1)–(5.5). The values and empirical correlations used to estimate the parameters in Eqs. (5.1)–(5.5) (e.g., dispersion coefficients), as well as additional parameters used in the model, are given in Table 5.1. Assuming that the concentration of bed material is equal to the bed density (i.e., $V_F << V_{BM}$), the velocity field of the bulk solids induced by the solids cross-flow is calculated from a potential flow function, Φ_{BM}, according to Eqs. (5.4a–b) [20].

Mass balance for gas species i in the bubble phase:

$$0 = \delta_b K_{be}\left(\rho_{G,e} Y_{e,i} - \rho_{G,b} Y_{b,i}\right) + S_{b,i} \tag{5.1}$$

Mass balance for gas species i in the emulsion phase:

$$0 = \delta_b K_{be}\left(\rho_{G,b} Y_{b,i} - \rho_{G,e} Y_{e,i}\right) + \frac{d}{dx}\left(D_G \rho_{G,e} \frac{dY_{e,i}}{dx}\right) + S_{e,i} \tag{5.2}$$

Mass balance of fuel component k of class j:

$$0 = -\frac{d}{dx}\left(\theta_{\mathrm{F}} u_{\mathrm{BM}} \rho_{k,j}\right) + \frac{d}{dx}\left(D_{\mathrm{F}} \frac{d\rho_{k,j}}{dx}\right) + S_{k,j} \tag{5.3a}$$

Potential flow model for the velocity field of bulk solids:

$$0 = \frac{d}{dx}\left(D_{\mathrm{BM}} \frac{d\Phi_{\mathrm{BM}}}{dx}\right) + S_{\mathrm{BM}} \tag{5.4a}$$

$$u_{\mathrm{BM}} = \frac{D_{\mathrm{BM}}}{\rho_{\mathrm{BM}}}\left(\frac{d\Phi_{\mathrm{BM}}}{dx}\right) \tag{5.4b}$$

Heat balance:

$$\begin{aligned} 0 = &-C_{\mathrm{p,BM}} \frac{d}{dx}\left(u_{\mathrm{BM}} \rho_{\mathrm{BM}} T\right) - \sum_k \frac{d}{dx}\left(\theta_{\mathrm{F}} u_{\mathrm{BM}} \rho_k h_{\mathrm{f},k}^{25\,^{\circ}\mathrm{C}}\right) + \sum_k \frac{d}{dx}\left(D_{\mathrm{F}} h_{\mathrm{f},k}^{25\,^{\circ}\mathrm{C}} \frac{d\rho_k}{dx}\right) \\ &+ \sum_i \frac{d}{dx}\left(D_{\mathrm{G}} \rho_{\mathrm{G,e}} \frac{dY_{\mathrm{e},i}}{dx}\left(h_{\mathrm{f},i}^{25\,^{\circ}\mathrm{C}} + C_{\mathrm{p},i}(T - 25\,^{\circ}\mathrm{C})\right)\right) + \frac{d}{dx}\left((k + k')\frac{dT}{dx}\right) + S_{\mathrm{E}} \end{aligned} \tag{5.5}$$

Table 5.1. Equations or values for the empirical parameters used in the model.

Parameter	**Value/equation**	**Reference**
D_{BM} (m^2/s)	$7.3\cdot10^{-3}\cdot u_0 + 1.3\cdot10^{-2}$	[73]
D_{F} (m^2/s)	$3.3\cdot10^{-2}\cdot u_0 - 4.0\cdot10^{-4}$	[45]
D_{G} (m^2/s)	10^{-4}	[74]
θ_{F} (–)	$\theta_{\mathrm{F}} \in [0,1]$ $4.7\cdot u_0 - 0.52$, $u_{\mathrm{BM}} = 0.009$ m/s $5.7\cdot u_0 - 0.63$, $u_{\mathrm{BM}} = 0.012$ m/s	[20] [20]
K_{be} (1/s)	$4.5\cdot\ (u_{\mathrm{mf}}/d_{\mathrm{b,av}}) + 5.85\cdot\ (D_{\mathrm{G}}^{0.5} g^{0.25}/d_{\mathrm{b,av}}^{1.25})$	[74]
d_{b0} (m)	$1.63[(u_0 - u_{\mathrm{mf}})\cdot A_0/g^{0.5}]^{0.4}$	[75]
d_{b} (m)	$0.54(u_0 - u_{\mathrm{mf}})^{0.4}\cdot(h + 4\cdot A_0^{0.5})^{0.8} g^{-0.2}$	[75]
$d_{\mathrm{b,av}}$ (m)	$[d_{\mathrm{b0}} + d_{\mathrm{b}}(h = H)]/2$	–
Re_{mf} (m/s)	$(33.7^2 + 0.0408Ar)^{1/2} - 33.7$	[76]
$\varepsilon_{\mathrm{mf}}$ (–)	$Ar = 1.75/(\varepsilon_{\mathrm{mf}}^3 \varphi_{\mathrm{BM}})\cdot Re_{\mathrm{mf}}^2$ $+150(1-\varepsilon_{\mathrm{mf}})/(\varepsilon_{\mathrm{mf}}^3 \varphi_{\mathrm{BM}}^2)\ \cdot Re_{\mathrm{mf}}$	[53]
δ_{b} (–)	$0.534 - 0.534\cdot\exp(-(u_0 - u_{\mathrm{mf}})/0.413)$	[77]
ε_{e} (–)	$0.62 - 0.059\cdot\exp(-(u_0 - u_{\mathrm{mf}})/0.429)$	[77]
k' (W/(m·K))	$D_{\mathrm{BM}}\cdot\rho_{\mathrm{BM}}\cdot(1-\varepsilon_{\mathrm{e}})\ \cdot C_{\mathrm{p,BM}} + D_{\mathrm{F}}\cdot\rho_{\mathrm{ash,bed}}\cdot C_{\mathrm{p,ash}}$	–

5.1.1. Mass Balances

Gas species

The gas species considered are CO, CO_2, H_2, H_2O, CH_4, and tar (represented by C_6H_6O). The gas flow is described by the two-phase model approach [78], which divides the gas into two phases: 1) the emulsion phase (containing the gas needed for minimum fluidization and all the solids); and 2) the bubble phase (containing all the excess gas fed to the bed, i.e., corresponding to a volumetric flux of $u_0 - u_{mf}$). Thus, for each gas species, two mass balances are formulated that correspond to the bubble phase [Eq. (5.1)] and the emulsion phase [Eq. (5.2)].

The first term on the right-hand-side (RHS) of Eqs. (5.1) and (5.2) describe mass transfer between the bubble phase and the emulsion phase, which is governed by the bubble-emulsion interchange coefficient, K_{be}. The second term in Eq. (5.2) describes the lateral gas transport within the emulsion phase, which is governed by the lateral gas dispersion coefficient, D_G. The final term in Eqs. (5.1) and (5.2) are the source terms, which include reactions (the water-gas-shift reaction) and transport into and out of the gasifier, i.e., the gas entering the reactor and that leaving at the bed surface.

It is assumed that drying and pyrolysis occur on the bed surface, which means that the gases released by these processes do not enter the bottom bed region. This behaviour has been confirmed for industrial-scale beds in the Chalmers gasifier using a hot-temperature camera probe [45], and it can to some extent be attributed to the lifting force of the endogenous bubbles formed around the fuel particles during pyrolysis [79].

Fuel

The reactive fuel components (moisture, volatiles, and char), k, are each divided into a number of classes, j, based on the degree of conversion (see Section 5.2), for all of which a mass balance [Eq. (5.3a)] is solved. Equation (5.3a) is also used to calculate the concentration field of ash within the gasifier, using only one class and no reaction terms.

Equation (5.3a) includes both convective and dispersive mass transport, as well as a source term that includes reactions and transport into and out of the gasifier. The convective transport is governed by the cross-flow impact factor, θ_F, which represents the extent to which the fuel particles follow the velocity field of the bed material induced by the solids cross-flow. For the cases in which a baffle-equipped gasifier (see Section 5.3) is used, the baffles are modelled by setting the dispersion coefficient, D_F, to a low value ($D_{F,low} = 10^{-6}$ m^2/s) and the cross-flow impact factor, θ_F, to zero at a certain grid surface.

As shown in Figure 5.1a, for a given fuel, a sub-model (see Section 5.2) is used to generate an interpolation table with values for the conversion rate of conversion class j of fuel component k ($R_{k,j}$) for a range of steam concentrations and/or temperatures, prior to the gasifier model simulations. In the gasifier model, the conversion rate of fuel species k of class j is then given at the cell steam concentration and/or temperature through interpolation.

The model of the gasifier takes into account the effects of operational conditions on the char gasification rate based on their influence on the axial distribution of fuel. This is achieved by determining the fraction of fuel particles that undergoes pyrolysis on the bed surface and char gasification inside the dense bed, $F_{BS/IB}$, according to the method described in **Paper III**, and by setting the char gasification rate at 50% lower than for all other fuel particles (results from **Paper IV**, see Section 6.1). The probability that pyrolysis occurs on the bed surface, and thus the value of $F_{BS/IB}$, increases with bed material velocity [45], which increases with scale (see Section 3.1). Thus, the char gasification rate will decrease with scale until $F_{BS/IB}$ reaches unity.

5.1.2. Heat Balance

In the gasifier model, a single heat balance [Eq. (5.5)] is solved, which includes both the gas and the solids (bed material and fuel). The difference in temperature between the fuel and the surroundings is accounted for with the particle model-based sub-model (described in Section 5.2). Furthermore, in Eq. (5.5), it is assumed that the reacting fuel components remain at the fuel inlet temperature until they are converted, whereas the ash and bed material are heated to the temperature of the bed.

The first and second terms on the RHS of Eq. (5.5) describe convective heat transfer by the bed material and the fuel, respectively. The third and fourth terms represent the heat transported by fuel and gas dispersion, respectively, whereas the fifth term designates the heat transfer due to temperature gradients, i.e., conduction, k, and that related to the dispersive mixing of bulk solids and ash, k' (see Table 5.1). The final (source) term represents the energy flows into and out of the gasifier, i.e., the feeding and outlet flows of fuel, bulk solids, and gas.

5.2. Conversion-Class Discretisation Method –Formulation

For each fuel components, Eq. (5.3a) can also be written in the form of a population balance according to:

$$\left\{\begin{matrix} rate\ of \\ accumulation \\ of\ class\ j \end{matrix}\right\} = \left\{\begin{matrix} net\ transport \\ rate\ of\ class\ j \end{matrix}\right\} + \left\{\begin{matrix} conversion \\ rate\ of \\ class\ j-1 \\ entering \\ class\ j \end{matrix}\right\} - \left\{\begin{matrix} conversion \\ rate\ of \\ class\ j \\ leaving \\ class\ j \end{matrix}\right\} \qquad (5.3b)$$

In Eq. (5.3b), the term on the left-hand side designates the rate of mass accumulation of a fuel component of class j within a computational cell. In this thesis, the focus is on steady-state conditions, so this term is set equal to zero. The first term on the RHS describes the net transport of class j of the fuel component due to mass transfer mechanisms, i.e., fuel convection and dispersion, or due to point sources/sinks (e.g., fuel feeding or draining).

In this thesis, the population balances used are based on the degree of conversion rather than on the size or density of the fuel particle. Thus, the second term on the RHS of Eq. (5.3b) describes how class j–1 of the fuel component (i.e., a class with a lower degree of conversion) enters class j

as a result of conversion, whereas the third term on the RHS designates the amount of the fuel component that leaves class j for a higher class, j+1, due to conversion.

Figure 5.2 outlines the principle of the conversion-based classes. Here, $\dot{m}_{j+1,k}$ designates the mass flow of fuel component k that has reached a certain degree of conversion, $X_{j+1,k}$, and thus leaves class j for class $j+1$.

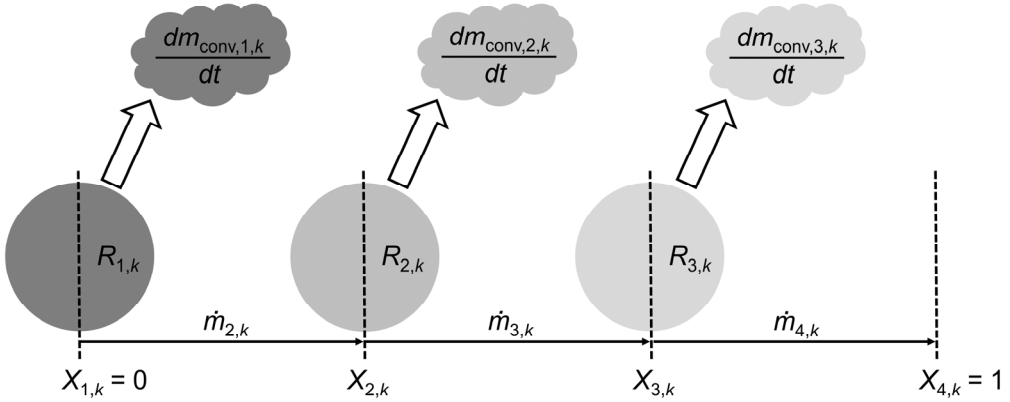

Figure 5.2. Principle of the conversion-based classes for three classes.

The mass flow of fuel component k leaving class j is given by:

$$\dot{m}_{j+1,k} = \frac{dm_{\mathrm{conv},j,k}}{dt} \cdot \frac{(1 - X_{j+1,k})}{(X_{j+1,k} - X_{j,k})} = R_{j,k} m_{k,0} \frac{(1 - X_{j+1,k})}{(X_{j+1,k} - X_{j,k})} \tag{5.6}$$

In this thesis, the conversion of a single fuel particle is simulated using a 1-dimensional transient model, which solves the energy and gas species transport equations and takes into account both the fuel conversion and shrinkage due to drying and pyrolysis. Moreover, the transfer coefficients in the particle model are corrected to account for the outflow of gases.

Running the particle model described above yields curves for the degree of conversion as a function of time. These curves can be discretised into a number of classes based on the conversion degree, for which each class (of size $\Delta X_{j,k}$,) has an individual conversion rate, $R_{j,k}$. Figure 5.3a shows the degree of pyrolysis at 800°C as a function of time, as given by the particle model, χ_k, and a linear approximation, $X_{\mathrm{lin},k}$, given by discretising the conversion process into three equally large classes, $\Delta X_{j,k}$ = 33% for j = 1–3. The shaded areas, $A_{j,k}$, signify the errors for classes j = 1–3.

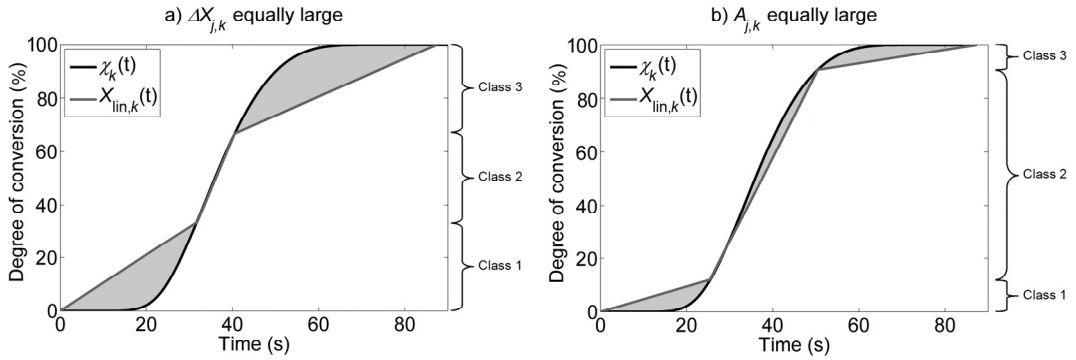

Figure 5.3. Degree of conversion as a function of time for the conversion of volatiles given by the particle model and a linear approximation using: a) three equally large classes; and b) the proposed discretisation method. The shaded areas represent the inaccuracies of the linear approximations.

As shown in Figure 5.3a, when three equally large classes are used, $A_{j,k}$ becomes very large for classes 1 and 3, and very small for class 2, resulting in a poor description of the conversion process. To decrease the error and distribute it uniformly along the conversion process, the areas between the curves for each class should be equally large. This is achieved using the discretisation method proposed in **Paper I**, which is based on making $A_{j,k}$ equal for all classes, as illustrated in Figure 5.3b.

The total error for fuel component k is defined according to Eq. (5.7), where P_k is a piece-wise polynomial representation of χ_k:

$$\varepsilon_k = \frac{\int_0^{t_{\text{tot},k}} \left| X_{\text{lin},k}(t) - P_k(t) \right| dt}{\int_0^{t_{\text{tot},k}} |P_k(t)| dt} \tag{5.7}$$

5.3. Modelled Cases

The cases modelled in this thesis can be divided into two categories: 1) cases that employ the dimensions and input data of the Chalmers gasifier; and 2) up-scaling and down-scaling simulations, for which the length-to-width ratio, bed height, and superficial fuel load in the gasifier (W/m^2) are the same as for the Chalmers gasifier (i.e., cross-sectional scaling is applied; see Section 2.2). The model input data for both types of simulations are given in Table 5.2.

The simulations of the Chalmers gasifier are used for model validation, as well as for investigating how operational conditions affect the dominant fuel mixing mechanisms (**Papers II** and **III** and Section 6.2.2). The validation data used are taken from Larsson et al. [1], Israelsson et al. [68], and Berdugo-Vilches et al. [69], all of whom conducted measurements in the Chalmers gasifier (see Section 5.3.1).

Table 5.2. Model input data.

Input parameter	Chalmers gasifier	Scaling simulations
P_{tot}	1.4–1.9 MW	1–420[a] MW
$Q_{cr} = \dot{m}_F LHV_F / A_{cross}$	1.0–1.3 MW/m^2	2 MW/m^2
L/W	2.25	2.25
Δp_{bed}	4–6 kPa	6 kPa
$T_{BM,in}$	700°–950°C	700°–900°C[b]
$T_{H2O,in}$	107°–250°C	200°–800°C[b]
$T_{F,in}$	25°C	25°C
SFR	0.2–1.4	0.3–1.0
$\dot{m}_{BM}/\dot{m}_F$	30–60	2–25
Fuel		
Type	Wood pellets	
Y_{moist} (as received)	9%	
Y_{ash} (as received)	0.5%	
Y_{char} (daf)	19%	
$Y_{C,char}$ (ash-free)	96%–100%	
$Y_{C,F}$ (daf)	51%	
$Y_{H,F}$ (daf)	6%	
$Y_{O,F}$ (daf)	43%	
LHV_F (as received)	16.9 MJ/kg	
LHV_{char} (ash-free)	30.5 MJ/kg	
d_F	8 mm	
ρ_F	1105 kg/m^3	
Char reactivity	From Lundberg et al. [80] and **Paper V**	
Bed material		
Type	Silica sand & activated olivine	
ρ_{BM}	2700 kg/m^3 & 3300 kg/m^3	
d_{BM}	292 µm & 490 µm	
φ_{BM}	0.86 (from Leva [81])	

[a] P_{tot} = 420 MW corresponds to the retrofit of a 100-MW combustor into a DFBG unit, given by Eq. (1.1) with $X_{char,g}^{opt}$ = 30% and the remaining parameters taken from Table 5.2.

[b] Unless stated otherwise, $T_{BM,in}$ = 900°C and $T_{H2O,in}$ = 200°C for the scaling simulations.

In the simulations used to investigate the effect of scale, DFBG units with capacities in the range of 1–420 MW$_{th}$ are modelled. Both new designs and retrofits of existing boilers into DFBG units

are considered. The effects of scale on the dominant fuel mixing regimes and the possibilities for process optimisation of DFBG units with different targets (solely gas production or heat and power production with gas as a by-product) are investigated (see Section 6.2.3). Two different gasifier designs are considered: 1) a base-case gasifier without any baffles; and 2) a baffle-equipped gasifier with baffles at $x/L = 0.2$ and 0.8.

All of the model simulations presented in the papers of this thesis were conducted using wood pellets and silica sand, as the available validation data at the time were based on this fuel and bed material, respectively. More recently, validation data have been obtained from experiments in the Chalmers gasifier using wood pellets and activated olivine as the fuel and bed material, respectively ([69], see Table 5.3). In this thesis, in addition to the studies described in the papers, the influences of an active bed material (activated olivine) on the degree of char gasification of wood pellets in the Chalmers gasifier (used for model validation) and in large-scale DFBG units are investigated. As there are no available reactivity data for the gasification of wood pellets in a bed of activated olivine, the process-assisted reactivity data for wood chip char in a bed of activated olivine, as determined in **Paper V** (see Table 6.2), are used. The structural parameters are set as being equal to those for fluidized bed steam gasification of wood pellets in silica sand, as given by Lundberg et al. [80].

5.3.1. Validation Data

Three sets of measurements conducted by Larsson et al. [1], Israelsson et al. [68], and Berdugo-Vilches et al. [69], respectively, in the Chalmers DFBG unit (see Figure 5.4) are used to validate the semi-empirical 1D model of the bottom bed of a BFB gasifier (described in Section 5.1). The unit consists of a 12-MW CFB combustor and a 2–4-MW BFB gasifier. Experimental data from the three aforementioned studies are listed in Table 5.3.

The degree of char gasification taken from Larsson et al. [1] was calculated from the carbon balance. The confidence interval (0%–10%) reflects uncertainties, primarily in the char yield (see Table 5.3). For the experiments conducted by Israelsson et al. [68] and Berdugo Vilches et al. [69], $X_{\mathrm{char,g}}^{\mathrm{meas}}$ was estimated from the carbon in the raw gas, which was measured after letting the raw gas pass through a high-temperature combustion reactor [82] that converted the gas to a mix of exclusively CO, CO_2, H_2, and H_2O:

$$X_{\mathrm{char,g}}^{\mathrm{meas}} = 1 - \frac{C_{\mathrm{F,daf}} - C_{\mathrm{G}}}{Y_{\mathrm{char}} \cdot Y_{\mathrm{C,char}}} \tag{5.8}$$

The uncertainty related to the char yield, as well as to the amount of carbon in the char (96% ± 4% [83]) yields a certain confidence interval for the values obtained using Eq. (5.8) (see Table 5.3). The amount of char circulated from the combustor to the gasifier is ignored, since it has been estimated as being rather low (0–0.12 $kg_{char,circ}/kg_{fed\ char,gasifier}$) [1].

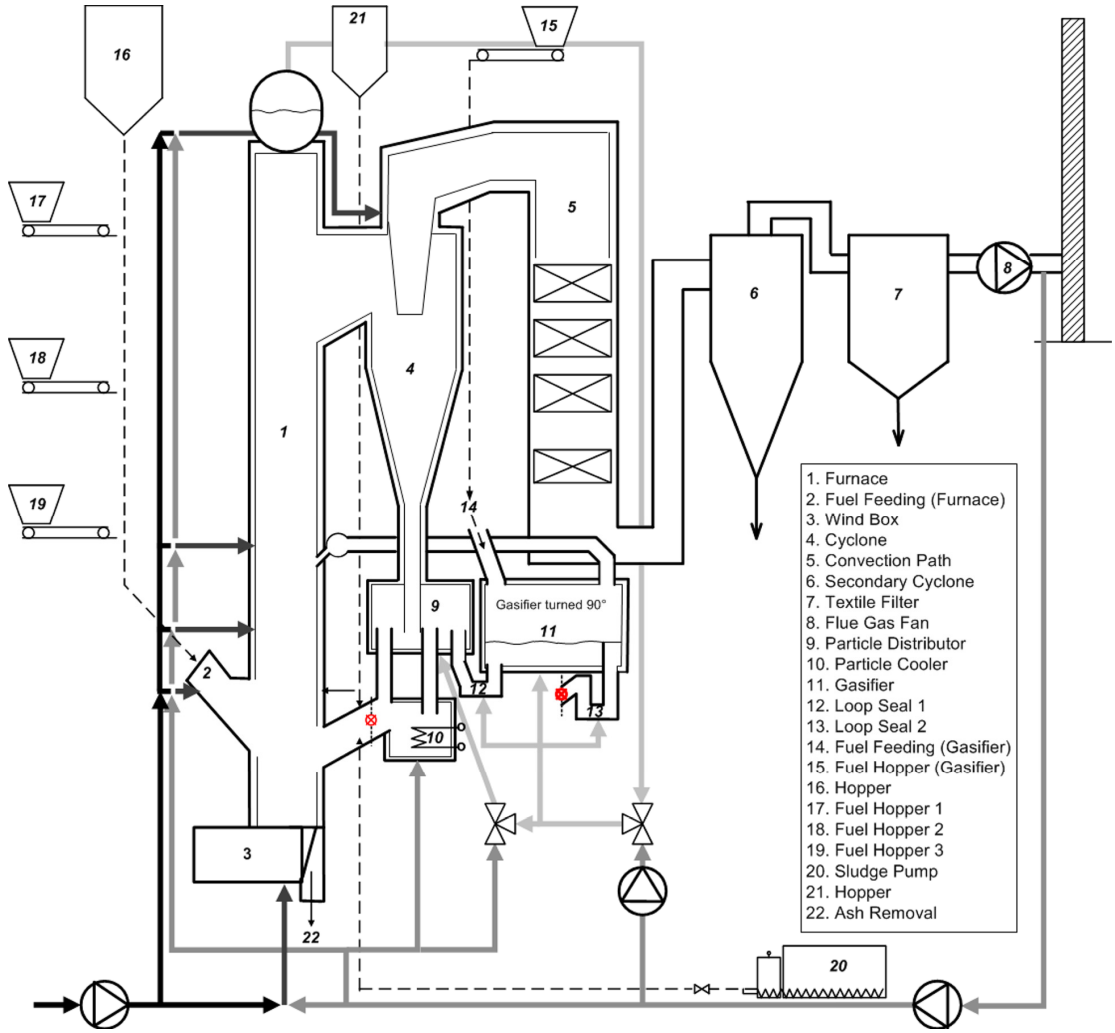

Figure 5.4. Schematic of the Chalmers DFBG system.

Table 5.3. Experimental data from the studies used to validate the gasifier model.

	Larsson et al. [1]	**Israelsson et al. [68]**	**Berdugo-Vilches et al. [69]**
No. of measurements used for validation	1	6	5
$\boldsymbol{T_{g,av}}$	830°C	782°–823°C	804°–829°C
$\boldsymbol{T_{H2O}}$	140°C	110°C	106°C
SFR	0.78 kg_{H2O}/kg_F	0.44–0.64 kg_{H2O}/kg_F	0.54 kg_{H2O}/kg_F
$\boldsymbol{\dot{m}_{BM}/\dot{m}_F}$	58 kg_{BM}/kg_F	31–35 kg_{BM}/kg_F	34–57 kg_{BM}/kg_F
Fuel	Wood pellets	Wood pellets	Wood pellets
Bed material	Silica sand	Silica sand	Activated olivine
Char yield	16% ± 2% (from [1])	19% ± 1% (from **Paper IV**)	19% ± 1% (from **Paper IV**)
$\boldsymbol{X_{char,g}^{meas}}$	2% (from [1])	Calculated from Eq. (5.8)	Calculated from Eq. (5.8)
Confidence interval	$X_{char,g}^{meas}$ = 0–10%	$X_{char,g}^{meas}$ ± 9%	$X_{char,g}^{meas}$ ± 9%
Plotted in figure(s)	Figure 6.9a	Figures 6.7 and 6.9a	Figure 6.8

6. Results and Discussion

6.1. Results from the Laboratory-Scale Experiments

Experiments were conducted in the laboratory-scale BFB gasifier (described in Section 4) to determine the effects of different parameters on char gasification. The results from the experimental work are summarised in Table 6.1. The uncertainties in the experimental data, as indicated by the error bars in Figure 6.1, are due to repetitions and uncertainties in the gas analysers and char yields. While these uncertainties are present for all the experimental results in this section, they are not shown in the remainder of the figures and tables in order to simplify the qualitative comparisons of different experiments.

Table 6.1. Summary of results from the experimental work. The third column gives the effect of the studied parameter on the char gasification rate, R_g, at $X_{char,g}$ = 20%.

Investigated parameter	**Details**	**Effect on $R_g(X_{char,g} = 20\%)$**	**Paper/Figure in thesis**
Pyrolysis atmosphere	N_2 vs. mixture of N_2 and H_2O	Negligible	**IV**/–
Batch size	5 vs. 10 wood pellets	Some effect, with R_g slightly higher for five pellets	**IV**/–
Fuel axial mixing	Four cases investigated, see Figure 6.1	Up to 2.0-fold lower for the BS/IB case	**IV**/Figure 6.1
Cooling after pyrolysis	Cooled char vs. non-cooled char	Up to 1.5-fold higher for non-cooled fuel	**IV**/–
Bed material	Silica sand vs. fresh olivine	Negligible	**V**/–
Bed material	Silica sand vs. activated olivine	Up to 2.0-fold higher for activated olivine	**V**/Figures 6.2 and 6.3
Bed material activation	Fresh vs. activated olivine	Up to 2.0-fold higher for activated olivine	**V**/–
Fuel moisture content	Moisture content (0%–40%)	Negligible	**V**/–
Fuel size	'Large', 'medium', and 'small' wood chips (see **Paper V**), with silica sand or activated olivine as bed material	Up to 2.0-fold higher for the small fuel particles	**V**/Figure 6.3
Fuel structure	Intact vs. crushed wood pellets	Up to 1.5-fold higher for crushed pellets	**IV**/Figure 6.4

As is evident from Table 6.1, the pyrolysis atmosphere, the fuel moisture content, and switching the bed material from fresh silica sand to fresh olivine all had negligible effects on the char gasification rate. The batch size had some effect on the char gasification rate, which is in line with previous studies (according to Qin and Thunman [30], at least 10 randomly picked pellets should be used to avoid batch variations). Cooling of the fuel after pyrolysis resulted in significantly lower

gasification rates compared to using non-cooled char, which is in agreement with previous studies (see for example, [24]).

Figure 6.1 shows the effects of fuel axial mixing during pyrolysis and char gasification on the char gasification rate. Pyrolysis on the bed surface and char gasification inside the dense bed (Case 3) result in a char gasification rate that is up to 2-fold lower than the corresponding rates for the other three cases. This is likely due to that the heat transfer to the fuel particles during pyrolysis is lower on the bed surface than inside the dense bed, whereas the level of steam-char contact during char gasification is lower inside the dense bed than on the bed surface. The combination of these two effects results in chars that are less porous and thus less reactive than chars that experience the conditions of any of the other three cases in Figure 6.1.

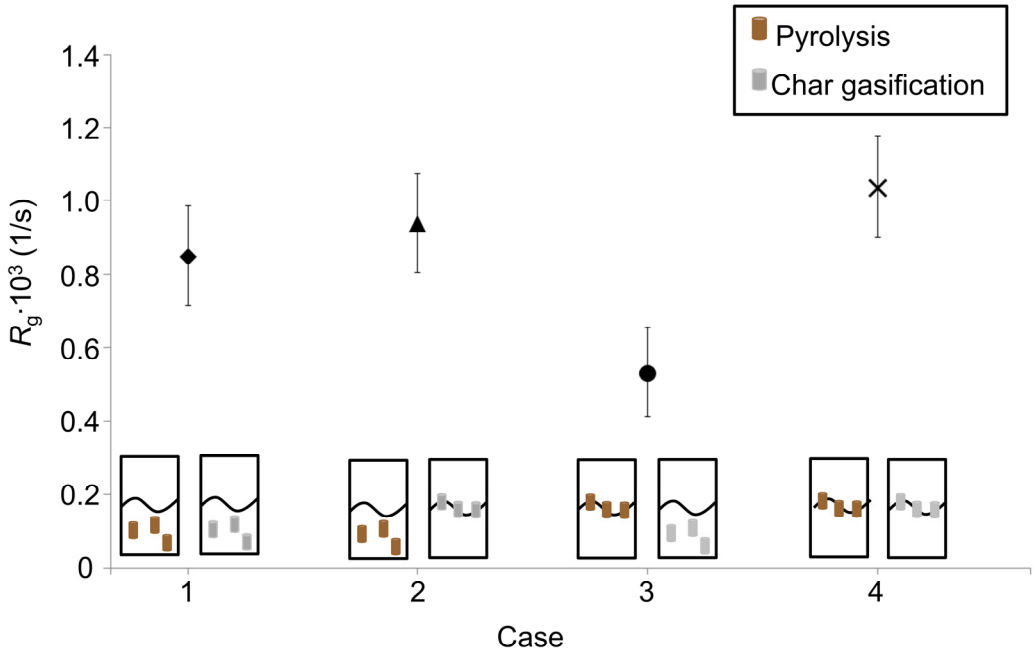

Figure 6.1. Effect of fuel axial mixing on the char gasification rate for wood pellets.

Figures 6.2 and 6.3 show the conversion profiles of wood chip chars at four temperatures and for three fuel particle sizes (large, medium, and small, see **Paper V** for size definitions), respectively, using silica sand or activated olivine as bed material. As shown in Figure 6.2, the char gasification rate is higher for activated olivine at all the temperatures applied owing to the catalytic effect of the ash layer covering the activated olivine particles.

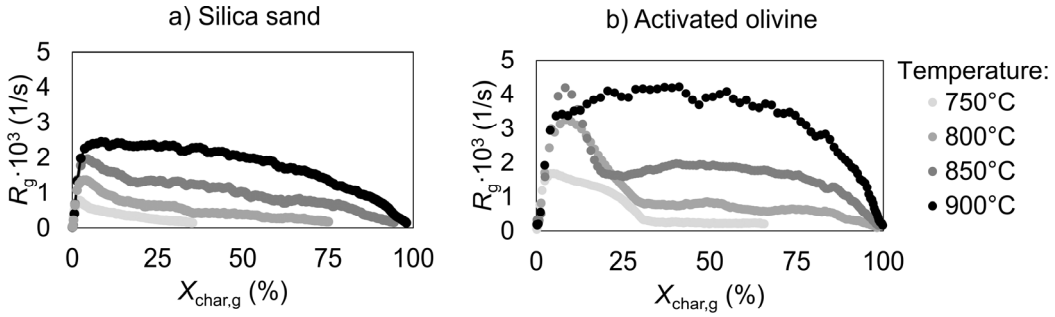

Figure 6.2. Char conversion profiles for small dry wood chips at 750°–900°C using two different bed materials: a) silica sand; and b) activated olivine.

Furthermore, as shown in Figures 6.2 and 6.3, the shape of the conversion profile (i.e., the variation of R_g with $X_{char,g}$) is affected by the choice of bed material. For silica sand the conversion profile shapes are similar for the four studied temperatures. However, for olivine, distinct peaks for R_g are observed for T = 750°–850°C, whereas this behaviour is not observed for T = 900°C.

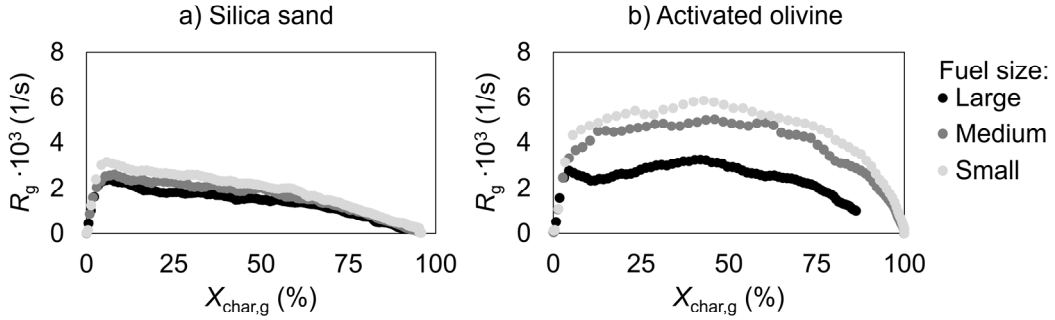

Figure 6.3. Char gasification rates for dry wood chips with three different fuel particle sizes and using two different bed materials: a) silica sand; and b) activated olivine.

The process-assisted kinetic parameters and reaction order of steam gasification of char from wood chips using either silica sand or activated olivine as the bed material are given in Table 6.2. It is clear that the choice of bed material strongly affects the activation energy. The observed effect is comparable to that linked to the intrinsic heterogeneity of ash content and composition in different biomasses. Furthermore, the reaction order, n, is slightly affected by the type of bed material used.

Table 6.2. Process-assisted kinetic parameters and reaction order for char from small wood chips at $X_{char,g}$ = 30% in beds of silica sand or activated olivine for T = 750°–850°C and p_{H2O} = 0.1–0.5 bar. For all the cases, $R^2 > 0.99$.

Bed material	k_0 **(1/(s·bar^n))**	E_a **(kJ/mole)**	n **(–)**
Silica sand	$5.6 \cdot 10^5$	181	0.6
Activated olivine	$5.5 \cdot 10^3$	137	0.5

The particle size of the wood chips has some effect on the char gasification rate, as depicted in Figure 6.3. This is likely due to mass transfer limitations, which decrease as the fuel particle size decreases. However, for both bed materials, the shape of the conversion profile is unaffected by fuel particle size. In contrast, for wood pellets, crushing the pellets has some effect on the shape of the conversion profile, as seen in Figure 6.4. In addition to a decrease in the mass transfer limitations as the fuel particle size decreases, this effect could be due to the fact that the crushed fuel is exposed to higher heating rates and a higher level of steam-fuel contact than the intact pellets, resulting in a more porous, reactive char.

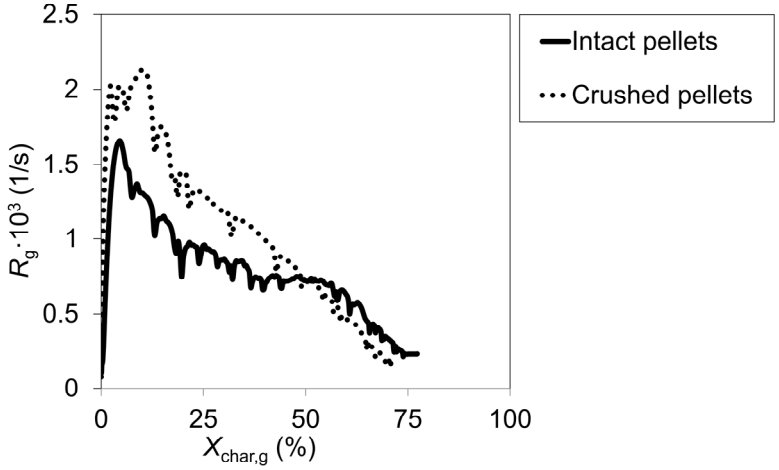

Figure 6.4. Char gasification rates for intact and crushed wood pellets.

The results presented above clearly demonstrate that that when designing laboratory-scale experiments to determine reactivity data destined for use in the modelling of biomass char gasification in fluidized beds, the conditions should ideally mimic those of the larger unit, which is in line with previous studies [25]. Thus, traditional methods, such as TGA, cannot be used. Instead, a laboratory-scale fluidized bed reactor should be employed. Furthermore, the following should be noted:

- Pyrolysis in an atmosphere of N_2 can be employed to separate pyrolysis from char gasification without compromising the validity of the results.
- A sufficiently high number of randomly picked fuel samples should be used.
- Dry fuel particles can be employed without significantly compromising the validity of the results.
- Relatively small fuel particle sizes should be used, although not if this demands that changes be made to the structure of the fuel particles (e.g., by crushing).
- The cooling of char particles after pyrolysis should be avoided.
- The same bed material (activated if non-inert) as that used in the large-scale unit should be employed.
- The effect of fuel axial mixing on the char reactivity should be accounted for in the design of the experiments and/or in the modelling.

6.2. Results from the Modelling Work

6.2.1. Performance of the Proposed Discretisation Method for Fuel Conversion

Figure 6.5 shows the total errors [defined in Eq. (5.7)] for the three stages of fuel conversion using: a) equally large classes; and b) the discretisation method based on the conversion degree proposed in Section 5.2. The proposed method results in errors up to 10-times lower than when using equally large classes, and for all fuel components, four classes are sufficient to yield errors of <5%.

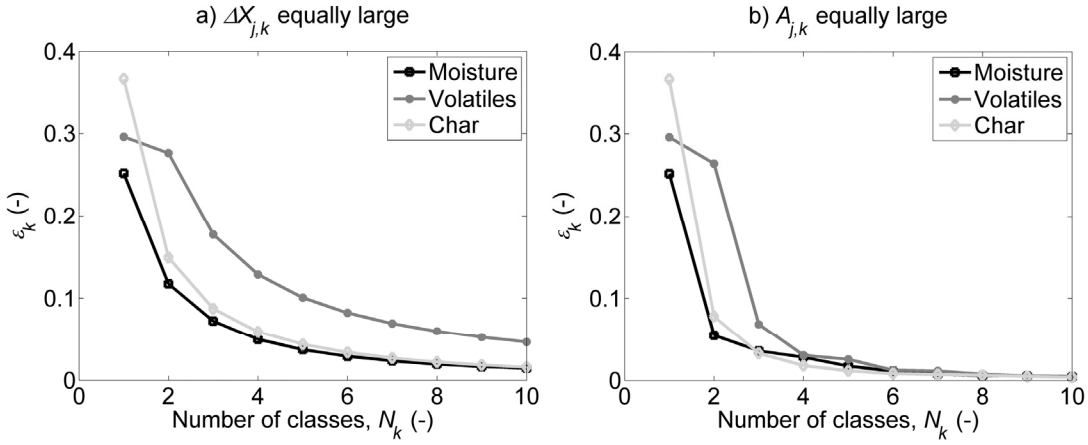

Figure 6.5. Errors as a function of the number of classes used for the three stages of fuel conversion at 800ºC for: a) when the $\Delta X_{j,k}$ values are equally high; and b) the proposed method with equally high values of $A_{j,k}$.

Figure 6.6 shows how the degree of char gasification converges as the number of conversion classes is increased when the proposed discretisation method is applied in the gasifier model used in this thesis, for DFBG units with capacities of 1 MW and 100 MW ($\dot{m}_{BM}/\dot{m}_F$ = 10). It is clear that when only one class is used the char gasification degree is strongly under-predicted. When 4–6 or more classes are used the change is less significant, which is in line with the results given in Figure 6.5b.

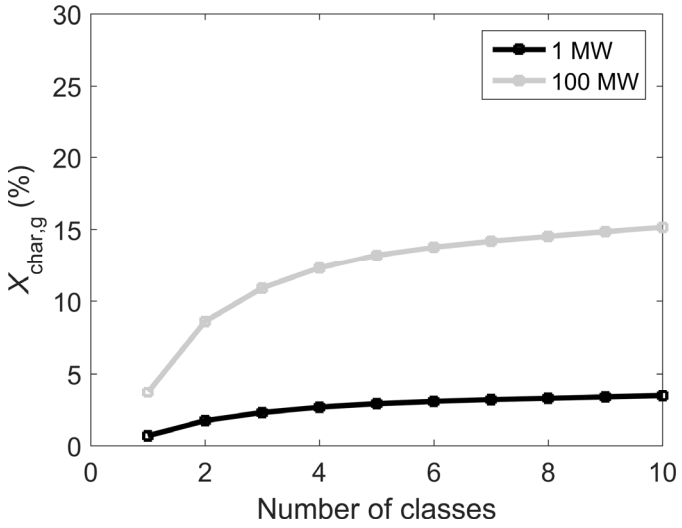

Figure 6.6. Convergence of the degree of char gasification as the number of classes is increased when the conversion-class discretisation method is applied in the gasifier model presented in this thesis for DGBG units of 1 MW and 100 MW.

6.2.2. Simulations of Char Gasification in the Chalmers Gasifier

In this section, the presented simulation results are based on the dimensions and input data of the Chalmers gasifier, using wood pellets as the fuel. The uncertainties associated with the measurements include those related to the char yield and the amount of C in the char, see Section 5.3.1.

The modelled and measured degrees of char gasification in the Chalmers gasifier for various bed material input temperatures and steam-to-fuel ratios are given in Figure 6.7, with silica sand as the bed material. As shown, the modelled degree of char gasification gives a satisfactory fit with the experimental data.

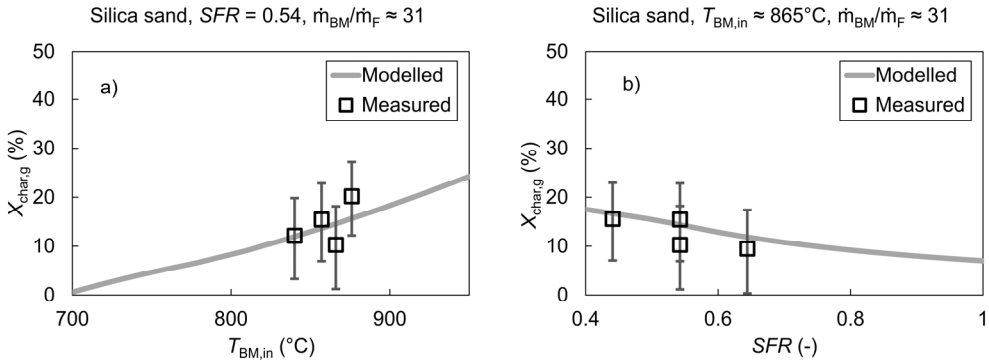

Figure 6.7. Using silica sand as the bed material, modelled and measured degree of char conversion in the Chalmers gasifier as a function of: a) the inlet temperature of the bed material; and b) the steam-to-fuel ratio.

As shown in Figure 6.7, both the experimental and modelled values of $X_{char,g}$ increase with the solids input temperature and decrease with the *SFR*. The fluidization velocity, u_0, and consequently the fuel lateral dispersion (D_F, see Table 5.1), increase with the *SFR*. Therefore, the observed decrease in $X_{char,g}$ with an increase in the *SFR* is caused by the decrease in fuel residence time as the fuel lateral dispersion increases.

Figure 6.8 shows the modelled and measured char gasification degrees in the Chalmers gasifier with activated olivine used as the bed material. The results of the model agree reasonably well with the experimental data, although the variations of the latter are larger than those observed for silica sand in Figure 6.7.

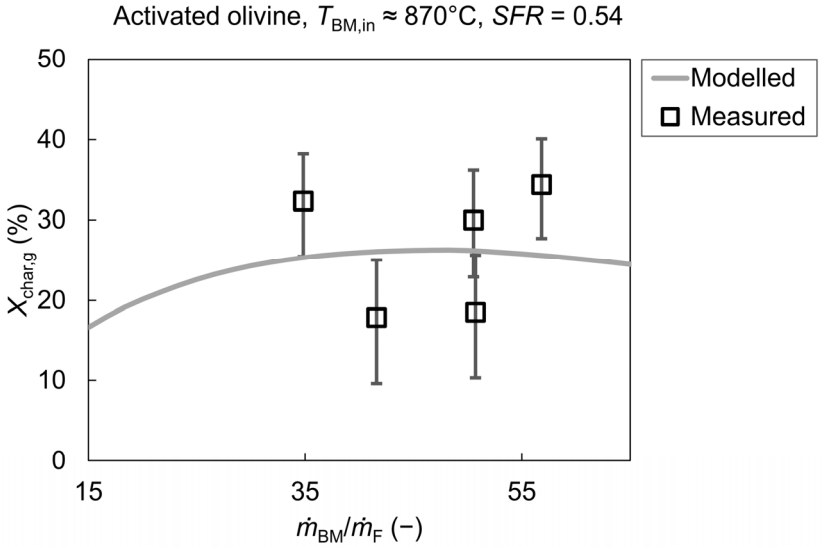

Figure 6.8. Measured and modelled degree of char conversion in the Chalmers gasifier as a function of the $\dot{m}_{BM}/\dot{m}_F$ ratio with activated olivine used as the bed material.

Regarding the degree of char gasification as a function of the fluidization velocity, Figure 6.9a shows modelled data for the Chalmers gasifier along with the data from two measurement points for two different solids cross-flows, with silica sand as the bed material. Figure 6.9b shows the boundary between the dispersion-dominant regime and the convection-dominant regime ($\tau_c = \tau_d$), as given by Eq. (3.4). To determine the dominant mixing regime for the cases modelled in Figure 6.9a, the property that governs fuel dispersion (the dispersion coefficient, D_F) is plotted against that governing fuel convection ($\theta_F \dot{m}_{BM}$; the cross-flow impact factor multiplied by the solids cross-flow) for each case modelled in Figure 6.9a (i.e., $\dot{m}_{BM}/\dot{m}_F$ = 31 and 58, and u_0 = 0.1–0.4 m/s).

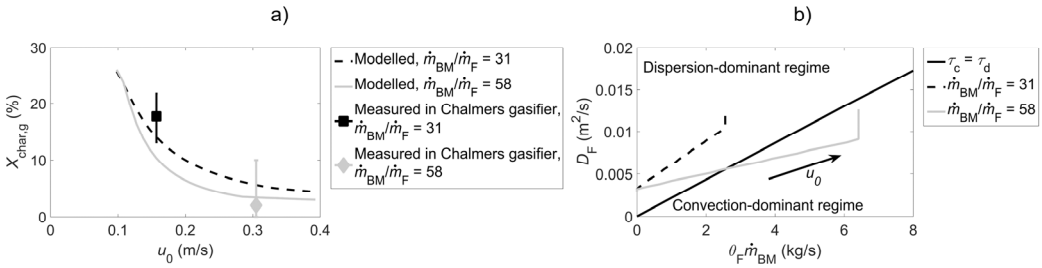

Figure 6.9. a) Degree of char conversion in the Chalmers gasifier as a function of the fluidization velocity for two different solids cross-flows with silica sand as the bed material; and b) the dominant mixing regimes for the cases modelled in a).

In Figure 6.9b, for both cases θ_F initially has a value of zero, which means that dispersion is the dominant fuel mixing mechanism. As u_0 increases, dispersion persists as the dominant mechanism for the lower solids cross-flow. In contrast, for the higher solids cross-flow, as the fluidization velocity increases (and hence θ_F, see Table 5.1), convection becomes the dominant fuel mixing mechanism. At a certain value of u_0 (in this case, 0.3 m/s), θ_F reaches its maximum value ($\theta_F = 1$), which results in a transition back towards the dispersion-dominant regime as u_0 increases further. This explains why $X_{char,g}$ in Figure 6.9a is the same for both solids cross-flows at $u_0 = 0.1$ m/s (i.e., $\theta_F = 0$) and why the curves start to converge at $u_0 \geq 0.3$ m/s (i.e., $\theta_F = 1$).

6.2.3. Scaling Simulations

In this section, the effects on the char gasification degree of up-scaling and down-scaling, and the possibilities for process optimisation are investigated for the two target modes presented in Section 1: 1) solely gas production; and 2) heat and power production, with gas generated as a by-product. The methods proposed to achieve process optimisation can be applied to both retrofits of existing CFB boilers into DFBG units and to newly designed DFBG units.

Figure 6.10 shows the degree of char conversion within the gasification chamber as a function of the $\dot{m}_{BM}/\dot{m}_F$ ratio for two values of the *SFR* for DFBG unit scales of 1 MW, 10 MW, 100 MW, and 420 MW, with wood pellets as the fuel and silica sand as the bed material. The fuel residence time [Eq. (3.1)] and the gasifier average temperature as functions of the $\dot{m}_{BM}/\dot{m}_F$ ratio are given in Figure 6.11 for a 100-MW DFBG unit with *SFR* = 0.4.

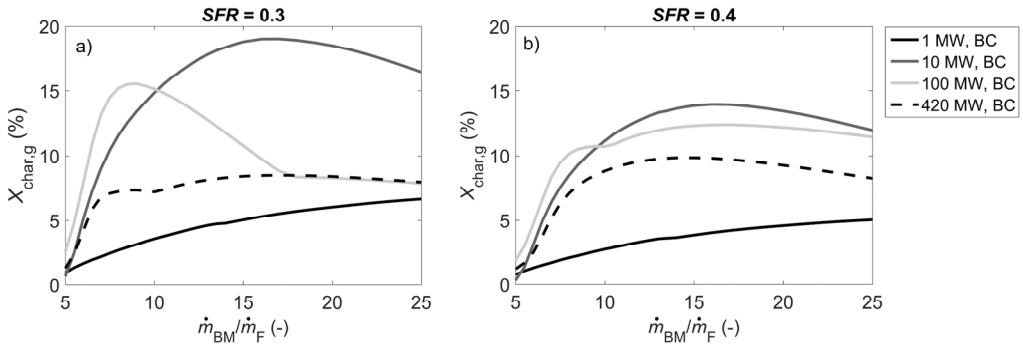

Figure 6.10. Degrees of char gasification for base-case gasifiers of 1 MW, 10 MW, 100 MW, and 420 MW, as a function of the $\dot{m}_{BM}/\dot{m}_F$ ratio for: a) SFR = 0.3; and b) SFR = 0.4.

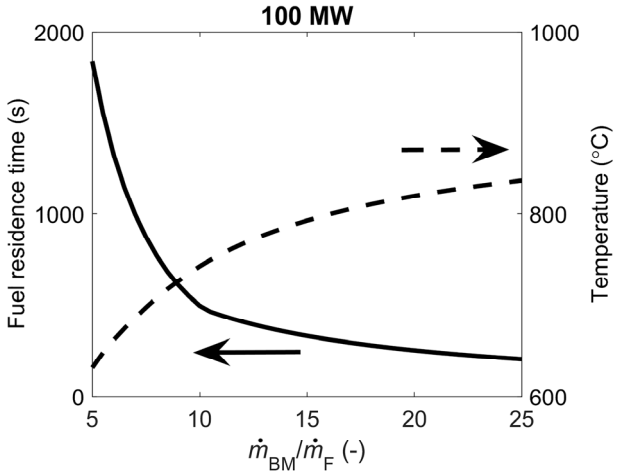

Figure 6.11. Fuel residence time [Eq. (3.1)] in relation to the average temperature within the gasifier for a 100-MW DFBG unit (SFR = 0.4).

As the curves for the temperature and the fuel residence time follow opposite trajectories with respect to the solids cross-flow (Figure 6.11), the degree of char gasification peaks at some value of the $\dot{m}_{BM}/\dot{m}_F$ ratio for all the scales, as shown in Figure 6.10. The extra peaks observed in two cases (420 MW, *SFR* = 0.3; and 100 MW, *SFR* = 0.4) reflect the sudden variation in the derivative of $\tau_F(\dot{m}_{BM}/\dot{m}_F)$, as observed in Figure 6.11, which makes the temperature effect on $X_{char,g}$ more dominant.

As the scale increases, τ_F (and thus $X_{char,g}$) initially increase. However, as discussed in Section 3.1, the bed material velocity increases with scale, creating a transition from the dispersion-dominant regime to the convection-dominant regime, which in turn leads to decreases in τ_F and $X_{char,g}$. In addition, increasing the bed material velocity increases the probability that pyrolysis occurs on the bed surface (see Section 5.1.1), where the level of heat transfer to the fuel particles is relatively low compared to that inside the dense bed, resulting in a less-reactive pore structure. This leads to a decrease in the char gasification rate, which contributes to the observed decrease in $X_{char,g}$ as the scale increases. Furthermore, as is evident in Figure 6.10, the influence of scale decreases as the

SFR is changed from 0.3 to 0.4, due to the fact that convection becomes more dominant as the *SFR* increases.

As discussed in Chapter 1, when DFBG is used exclusively for gas production, at a certain value of the degree of char gasification (typically in the range of 10%–50%) there is an optimum in the overall efficiency [1]. As shown in Figure 6.10, for the base-case gasifier with silica sand as bed material, it may be difficult to achieve sufficiently high levels of char gasification. If this is the case, a combination of optimised operational conditions, an active bed material, and the incorporation of baffles into the gasifier results in significant increases in the degree of char gasification (Table 6.3).

Table 6.3. Degrees of char gasification for the base-case gasifier and the baffle-equipped gasifier for different bed materials, steam-to-fuel ratios, and temperatures of the steam entering the gasifier. For all cases, $\dot{m}_{BM}/\dot{m}_F = 10$.

Gasifier design	***SFR*** **(kg/kg)**	T_{H2O} **(°C)**	Bed material	$X_{char,g}$ **(%)**
Base case	0.4	200	Silica sand	11
Base case	0.3	200	Silica sand	15
Base case	0.4	200	Activated olivine	20
Baffle-equipped	0.4	200	Silica sand	23
Baffle-equipped	0.4	200	Activated olivine	36
Baffle-equipped	1	800	Silica sand	47
Baffle-equipped	1	800	Activated olivine	67

In contrast, if heat and power production is the main target, with gas generated as a by-product, the degree of char gasification should be close to zero so as to minimise the heat demand in the gasifier. Figure 6.12 shows the degrees of char gasification and pyrolysis for solids input temperatures of 900°C (a typical temperature for CFB combustors) and 700°C (below which the level of char gasification is negligible) for DFBG units with capacities of 1 MW and 100 MW.

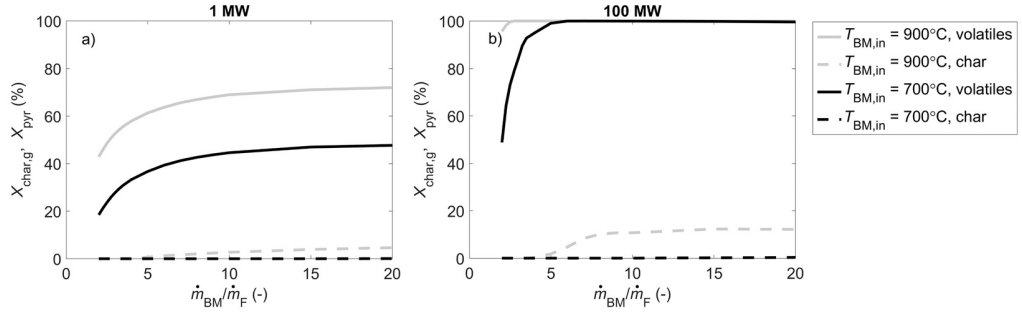

Figure 6.12. Degrees of char gasification and pyrolysis as a function of the $\dot{m}_{BM}/\dot{m}_F$ ratio for different input temperatures in: a) a 1-MW gasifier; and b) a 100-MW gasifier.

As depicted in Figure 6.12, for the small-scale base-case gasifier, the fuel residence time becomes too short to achieve complete pyrolysis (i.e., $X_{pyr} < 1$). Increasing $T_{BM,in}$ from 700°C to 900°C results in not only a higher level of pyrolysis, but also an increase in char gasification. For larger units, however, complete pyrolysis ($X_{pyr} = 1$) is easily achieved at low solids cross-flows, even at low temperatures, due to the long fuel residence time (Figure 6.12b). At high temperatures, a significant amount of char is also converted.

6.3. Discussion

6.3.1. Process Optimisation

As shown in Section 6.2.3, when heat and power production is the main target with gas generated as a by-product, process optimisation, i.e., complete pyrolysis and a low level of char gasification, can be achieved for large-scale units by adjusting the operational conditions. However, as demonstrated in Figure 6.12a, for smaller gasifiers, this may lead to incomplete pyrolysis, so the fuel residence time needs to be increased, e.g., by inserting baffles in the reactor. The use of baffles also allows for a smaller gasifier. For both small and large scales, $T_{BM,in}$ and/or the solids circulation should be limited, so that the gasifier temperature is kept sufficiently low to avoid char gasification. This can be achieved with a by-pass system for the solids (exemplified by the Chalmers DFBG unit, see Section 2.2) and/or an external heat exchanger being located prior to the gasification chamber.

If instead the main target is solely gas production, $X_{char,g}^{opt}$ is the minimum acceptable value for the degree of char gasification, so the temperature within the gasification chamber should be relatively high. As described in Section 6.2.3, in this case, in addition to adjusting the operational parameters, baffles will probably be needed to attain sufficient levels of char conversion within the gasification chamber. An alternative to using baffles could be to use an active bed material, such as olivine. However, if high char gasification degrees are desired, as could be the case if the end-product requires a raw gas with high concentrations of CO and H_2 (e.g., Fischer-Tropsch diesel, see Section 1), a combination of baffles and an active bed material are likely to be necessary.

For a DFBG system that has been designed for heat and power production, it is generally difficult to switch the operation mode to target gas production. This is because the relatively small gasifier that is used to yield the fuel residence times necessary for complete pyrolysis does not allow for significant levels of char gasification. As for DFBG units that are designed for gas production, their operation can be switched to target heat and power production (with gas as a by-product) by decreasing the temperature within the gasifier, such that char gasification is avoided (e.g., by by-passing a suitable fraction of the solids circulation flow).

Poly-generation units, i.e., those that have a flexible output with controllable shares of heat, power and gas, should follow the design guidelines for units devoted to gas production, namely a large gasifier (enabling a sufficient fuel residence time for char gasification when needed in the gas production mode) and the possibility to control the flow and/or temperature of the solids flow

entering the gasifier (e.g., by means of a by-pass system or an external heat exchanger located prior to the gasification chamber).

6.3.2. Model Assumptions

As described in Section 5.1, the velocity field of the solids within the gasifier is calculated from a potential flow function, which requires the assumption that the volume of fuel within the gasifier is much smaller than the volume of bed material. This is a reasonable assumption; for most of the simulations in this thesis, the volume of fuel within the system is <5% of the total bed volume.

Furthermore, it is assumed that the velocity field within the gasifier is uniform, and that the solids leave the gasifier by falling over the edge at the outlet. The first of these assumptions is reasonable for gasifiers of rectangular geometry, such as the Chalmers gasifier. Furthermore, in the Chalmers gasifier, the solids leave the gasifier in accordance with the second assumption. Thus, for systems with a geometry similar to that of the Chalmers gasifier, it is reasonable to model the gasifier using only one dimension, that of the solids cross-flow. However, for a gasifier with a circular cross-section, and with a solids outlet below the bed surface, such as the GoBiGas gasifier, this approach would not be valid. In that case, it is likely that a 3D approach is necessary to yield reliable results.

In the modelling, it is assumed that char gasification occurs in the emulsion phase of the dense bed and that drying and pyrolysis occur on the bed surface, such that the volatile gases do not enter the dense bed. This has two implications: 1) the concentration of steam within the emulsion phase becomes higher than if pyrolysis were to occur within the emulsion phase. However, assuming that drying and pyrolysis occur on the bed surface also means that the steam that originates from the fuel moisture and volatiles does not enter the bottom bed. For a fuel with a high moisture content, such as wood chips, this could instead result in an under-prediction of the steam concentration within the emulsion phase; and 2) the only species causing volatiles inhibition are the CO and H_2 produced during char gasification, since the volatiles do not enter the bed. Both these factors result in an over-estimation of the char gasification rate if pyrolysis in fact occurs within the dense bed. Moreover, the model does not explicitly account for volatiles inhibition (n^{th}-order kinetics are assumed). However, for the determination of the kinetic data for char gasification used in this thesis using the laboratory-scale fluidized bed gasifier described in Chapter 4 (see [80] and **Paper V**), the inhibitory effects of H_2 and CO are included indirectly, as these species are present in the dense bed during char gasification in the experiments.

As discussed in Section 5.1.1, the probability that pyrolysis occurs on the bed surface was found to be relatively high in the Chalmers gasifier at moderate fluidization velocities, and this probability increased with the bed material velocity. Thus, for large-scale gasifiers, where the bed material velocity is relatively high for the geometrical assumptions made in this thesis, it is reasonable to assume that a high proportion of the particles undergo pyrolysis on the bed surface. Furthermore, for large reactors, pyrolysis occurs close to the inlet whereas char gasification occurs throughout the reactor. Therefore, regardless of the axial position of pyrolysis, the influence of volatiles on char gasification is likely to be rather weak in most parts of the reactor. However, for smaller

gasifiers, pyrolysis and char gasification are likely to occur at the same locations within the reactor, and as the bed material velocity decreases with scale, pyrolysis is more likely to occur inside the dense bed. Therefore, for small-scale gasifiers, the model somewhat over-estimates the char gasification rate and consequently, the resulting degree of char gasification.

The two-phase model is used to model the gas flow, as mentioned in Section 5.1.1. This rather simple approach was chosen over more complex approaches (e.g., the inclusion of a cloud phase) because the gas concentration fields are not resolved in the axial direction and the literature lacks bubble-emulsion inter-phase coefficients for large-scale units. Thus, additional details would add complexity to the model without increasing the reliability of the results.

As mentioned in Section 5.2, the particle model includes shrinkage due to drying and pyrolysis. However, the effects of char shrinkage and char fragmentation are not accounted for by the model. In **Paper IV**, where wood pellets were subjected to steam gasification in a laboratory-scale fluidized bed, no significant char fragmentation or char shrinkage was observed for a char gasification degree of 62%. Thus, for the degrees of char gasification relevant to this thesis ($X_{\text{char,g}} \leq 67\%$), it is reasonable to ignore these phenomena for wood pellets.

As mentioned in Section 5.3, given the lack of experimental reactivity data on the gasification of wood pellets in activated olivine, for the simulations of this combination of fuel and bed material conducted within this thesis, the kinetics of wood chips in activated olivine and the structural parameters for wood pellets in silica sand were employed. For the purposes of this thesis (to qualitatively investigate how bed material activation affects the degree of char gasification in large-scale DFBG units), this is deemed to be a reasonable simplification, since wood chips and wood pellets have very similar compositions. However, as the fuel structure affects the char reactivity and the choice of bed material influences how the char reactivity changes with the degree of char gasification (Section 6.1), when the modelling results are to be used in the design, retrofitting, up-scaling, control, or optimisation of DFBG units, it is essential that the kinetic and structural data have been determined for the correct combination of fuel and bed material (activated if non-inert).

6.3.3. Analysis of the Papers over Time

As mentioned in Section 1.2, the model presented in this thesis (and in **Paper II**) has evolved over time and has been continuously refined with new knowledge gained from the experimental and modelling investigations presented in the papers. Originally, the fuel conversion was modelled using simpler means (the 0-dimensional approach for drying and pyrolysis, and the shrinking sphere approach with literature data for wood kinetics for char gasification; see [72]).

Laboratory-scale experiments using wood pellets and silica sand were carried out to determine the kinetic parameters for char gasification (described in Lundberg et al. [80], not included in this thesis), and to investigate, along with other parameters, the effect of the fuel axial mixing on the char gasification rate (**Paper IV**). Fuel axial mixing (Figure 6.1) was identified as an important parameter and was incorporated into the gasifier model (**Paper III**). Furthermore, after identifying the need for a more generic method to describe the discretisation of the fuel conversion, the

discretisation method presented in **Paper I** was developed and was, together with the reactivity data obtained in Lundberg et al. [80], incorporated into the model of the gasifier in the form of a sub-model. Finally, the effect of bed material activation on char reactivity was incorporated into the model using the reactivity data for wood chips and activated olivine described in **Paper V**.

As mentioned above, wood pellets and silica sand were employed as fuel and bed material, respectively, in **Paper IV**, in the char reactivity study described in Lundberg et al. [80], and in all of the simulations conducted in the papers related to this thesis. Wood pellets and silica sand were chosen for the sake of simplicity, and because the available validation data and reactivity data at the time of the simulations were based on this fuel and bed material. Furthermore, wood pellets have a relatively high density and it is more challenging to separate pyrolysis from char gasification for wood pellets than for other fuels, such as wood chips or forest residues. This ensures that the degree of char conversion in the gasification chamber is not over-estimated.

Given the current state-of-the-art, it is very likely that the bed materials applied in DFBG units will be active materials, such as olivine. Thus, the relevance of the experimental and modelling studies conducted in **Papers I–IV** would have been higher if activated olivine had been used as the bed material instead of silica sand. Furthermore, if validation data had been available, cheaper fuels, such as forest residues, could have been employed in the experimental and modelling studies.

As mentioned in Section 5.3, validation data obtained through measurements using activated olivine and wood pellets in the Chalmers gasifier have become available recently. For this reason, in addition to the results presented in the papers, this thesis includes results from simulations based on the reactivity data for wood chips with activated olivine as bed material (from **Paper V**).

7. Conclusions

In this thesis, key knowledge gaps are identified and filled regarding how different parameters influence solid fuel conversion in the gasification chamber of a DFBG unit, through the use of a combination of semi-empirical modelling and laboratory-scale experiments. The findings are used to propose methods that can be used for the design, up-scaling, retrofitting, optimisation, and control of such units.

The conducted laboratory-scale experiments show that fuel axial mixing significantly influences the char gasification rate. Furthermore, the choice of bed material strongly affects both the kinetic parameters and the shape of the char conversion profile (i.e., the variation of reactivity with the degree of char gasification). In contrast, the moisture content of the wood chips has a weak effect on the char gasification rate. The shapes of the char conversion profiles differ for crushed wood pellets and intact pellets, whereas they are very similar for wood chips of different sizes.

The experimental findings reported in this thesis corroborate the notion that experimental determination of reactivity data at the laboratory scale should mimic as closely as possible the conditions of the end-scale reactor to be modelled. Thus, traditional methods, such as TGA, cannot be used. Instead, a fluidized bed reactor should be employed, using the same bed material as that used in the large-scale unit (activated if non-inert), and the size of the fuel particles used should be as small as possible to avoid mass transfer limitations without compromising the structure of the fuel (e.g., by crushing pellets).

A validated, semi-empirical 1D model of the gasification chamber of a DFBG unit has been formulated, which accounts for the effect of fuel axial mixing on the char gasification rate. Furthermore, a computationally efficient method for describing fuel conversion in fluidized beds, which can be used to model different fuels with various size distributions and which is valid regardless of the fuel conversion regime, has been developed and verified.

The scale of the DFBG unit strongly affects the dominant fuel mixing regime. Initially, for small scales, fuel dispersion is dominant. Increasing the scale (and thus, the size) results in a longer fuel residence time. However, for the assumptions made in this thesis regarding scaling, the significance of fuel convection increases as the scale is increased due to the fact that the bed material velocity increases with scale. The increase in bed material velocity with scale also makes it more likely that the fuel particles will undergo pyrolysis on the bed surface where the heat transfer to the fuel particles is relatively low. This results in a less-reactive pore structure of the char, which contributes to a decrease in the degree of char gasification as the scale increases.

The natural initial increase in fuel residence time caused by the up-scaling process results in satisfactory fuel conversion when heat and power are the main products, with gas generated as a by-product. However, when gas production is the main target, additional measures, e.g., a combination of baffles, an active bed material, and appropriate operational conditions, are likely required to achieve sufficient fuel conversion in the gasification chamber.

A poly-generation unit, which can be switched between the two aforementioned product modes, should be designed with a relatively large gasifier to achieve the fuel residence times required for sufficient char gasification when gas is the main product. Furthermore, to achieve the low gasifier temperatures required in the heat and power production mode, the unit should have an external heat exchanger located prior to the gasification chamber and/or be designed so that a portion of the solids can by-pass the gasification chamber.

8. Future Work

This thesis has investigated how fuel conversion, and in particular the degree of char conversion ($X_{char,g}$), within the gasification chamber of a DFBG unit can be controlled and predicted for different operational conditions and gasifier sizes. The value of $X_{char,g}$ is determined by two factors: 1) the char gasification rate; and 2) the fuel residence time.

The char gasification rate is studied extensively in this thesis, and even though knowledge gaps remain (e.g., regarding the effect on char reactivity of volatiles inhibition in combination with an active bed material), the understanding of this parameter can now be considered sufficient to allow reliable predictions of how it is influenced by the operational conditions, gasifier scale, fuel properties, and bed material properties in a DFBG unit.

Regarding the fuel residence time, the results from this thesis show that to achieve process optimisation of a DFBG unit with gas as the sole product, it is crucial that the fuel residence time can be controlled, e.g., using baffles, or alternatively setting the fuel outlet below the bed surface. The modelling of baffles in this thesis is highly simplified, with zero- and one-dimensional descriptions of the baffles and the bed, respectively. As a baffle forces the fuel particles to mix in the axial direction to allow flow towards the reactor outlet, the impacts of baffles on $X_{char,g}$ described in this thesis should be regarded as an indication of the potential of baffles rather than an accurate quantitative analysis of their effects.

In order to gain a better understanding of the effects of baffles, and to investigate the optimal design, number, and locations of the baffles, a 3D model should be applied to enable modelling of fuel movements in the axial direction. 3D modelling may also be needed to accurately describe the fuel conversion for certain gasifier designs. For instance, in the GoBiGas gasifier, as the fuel outlet is located below the bed surface, the fuel residence time is largely governed by fuel axial mixing, which cannot be modelled with the 1D model. Furthermore, a 3D model would allow for optimisation of the gasifier design (e.g., the locations and designs of the inlets and outlets). In addition, 3D modelling would enable evaluation of the accuracy of 1D modelling with respect to the description of different phenomena.

As mentioned in Section 1, in the future it is expected that poly-generation units, which can switch the production focus between gas production and heat and power production (with gas as a by-product), will become more common. Therefore, future research on the optimisation of fuel conversion in DFBG units should focus on how this can be achieved for both production modes in a poly-generation unit under different conditions (e.g., variable loads and fuel types).

Notation

Roman letters

A_0	bed cross-section/number of holes (m^2)
A_{cross}	cross-section of gasifier (m^2)
A_j	error of class j (s)
Ar	Archimedes number (–)
C	mass of carbon per kg daf fuel ($kg/kg_{F,daf}$)
C_p	heat capacity (J/(kg·K))
D	dispersion coefficient (m^2/s)
d	diameter (m)
E_a	activation energy (J/mol)
$F_{pyr/char,g}$	fraction of fuel particles (–)
$f(X_{char,g})$	structural model (–)
g	gravitational acceleration (m/s^2)
H	bed height (m)
h	axial position in bed (m)
$h_f^{25°C}$	heat of formation at 25°C (J/kg)
k	thermal conductivity (W/(m·K))
k'	dispersion heat transfer coefficient (W/(m·K))
k_0	pre-exponential factor ($1/(s \cdot bar^n)$)
K_{be}	bubble-emulsion inter-phase coefficient (1/s)
L	gasifier length (m)
LHV	lower heating value (MJ/kg_F)
m	mass (kg)
$\dot{m}$	mass flow (kg/s)
$m_{C,0}$	initial carbon mass (kg)
$m_C(t)$	carbon mass at time t (kg)
$m_{F,0}$	initial dry fuel mass (kg)
n	reaction order (–)
P	piece-wise polynomial representation of χ (%)
Δp_{bed}	pressure drop over bed (Pa)
P_{comb}	combustor fuel demand (MW)
p_{H2O}	steam partial pressure (bar)
P_{tot}	total fuel input to DFBG unit (MW)
Q_{cr}	superficial fuel load in gasifier (W/m^2)
R	reactivity/conversion rate (1/s)
R	gas constant (J/(mol·K))
Re	Reynolds number (–)
R_g	gasification rate (1/s)
S	source term (depends on equation)
SFR	steam-to-fuel ratio (kg/kg_F)
T	temperature (ºC)
t	time (s)
u	velocity (m/s)
u_0	fluidization velocity (m/s)
V	volume (m^3)
W	gasifier width (m)
X	degree of conversion (%)
x	space coordinate of discretisation (m)
ΔX_j	size of conversion class j (–)
Y	mass fraction (kg/kg)
Y_{ash}	ash content (kg/kg_F)
Y_{char}	char yield ($kg/kg_{F,daf}$)
Y_i	mass fraction of gas species i (kg/kg)
Y_{moist}	moisture content (kg/kg_F)

Greek letters

δ	volume fraction (–)
ε	voidage (–)
ε_k	total error for fuel component k (–)
η	efficiency (–)
θ	cross-flow impact factor (–)
ρ	concentration, density (kg/m^3)
τ	residence time, time-scale (s)
Φ	potential flow function (kg/m^3)
φ	sphericity (–)
χ	conversion degree in particle model (%)

Indices

0	initial
av	average
b	bubble
BM	bed material
C	carbon
c	convective
char,g	char gasification
conv	conversion
d	dispersive
daf	dry ash-free
E	energy
e	emulsion
F	fuel
G	gas
g	gasifier
H	elemental hydrogen
H_2O	steam
i	gas species
in	inlet
j	conversion class
k	fuel component
lin	linear approximation
meas	measured
mf	minimum fluidization
O	elemental oxygen
opt	optimal
pa	process-assisted
pyr	pyrolysis
tot	total

Acronyms

BECCS	bio-energy carbon capture and storage	FBG	single fluidized bed gasification
BFB	bubbling fluidized bed	IB	inside dense bed
BS	bed surface	LPT	Lagrangian particle tracking
CFB	circulating fluidized bed	RHS	right-hand-side
CFD	computational fluid dynamics	SFR	steam-to-fuel ratio
DFBG	dual fluidized bed gasification	SNG	substitute natural gas
DME	dimethyl ether	TGA	thermogravimetric analysis
EFG	entrained flow gasification		

References

[1] Larsson, A., Seemann, M., Neves, D., Thunman, H. Evaluation of performance of industrial-scale dual fluidized bed gasifiers using the Chalmers 2-4-MWth gasifier. *Energy and Fuels*, 2013, 27, 6665-6680.

[2] IPCC. Climate Change: The IPCC Scientific Assessment. Cambridge University Press, Cambridge, 1990.

[3] European Union. Paris Agreement. https://ec.europa.eu/clima/policies/international/negotiations/paris_en, 2015.

[4] Trafikverket. Transportsektorns utsläpp. http://www.trafikverket.se, 2018.

[5] Gustavsson, L., Holmberg, J., Dornburg, V., Sathre, R., Eggers, T., Mahapatra, K., Marland, G. Using biomass for climate change mitigation and oil use reduction. *Energy Policy*, 2007, 35, 5671-5691.

[6] Azar, C., Lindgren, K., Obersteiner, M., Riahi, K., van Vuuren, D.P., den Elzen, K.M.G.J., Möllersten, K., Larson, E.D. The feasibility of low CO2 concentration targets and the role of bio-energy with carbon capture and storage (BECCS). *Climatic Change*, 2010, 100, 195-202.

[7] Hofbauer, H. Scale Up of Fluidized Bed Gasifiers from Laboratory Scale to Commercial Plants: Steam Gasification of Solid Biomass in a Dual Fluidized Bed System. FBC19, Vienna, Austria, 2006.

[8] Neubauer, Y. 6 - Biomass gasification. In: Rosendahl, L. (Ed.), Biomass Combustion Science, Technology and Engineering, Woodhead Publishing, 2013, pp. 106-129.

[9] Larsson, A. Fuel conversion in a dual fluidized bed gasifier -experimental quantification and impact on performance. Doctoral Thesis, Energy and Environment, Chalmers University of Technology, Göteborg, Sweden, 2014.

[10] Zuideveld, P.L., de Graaf, J. Overview of Shell global solutions' worldwide gasification developments. Gasification Technologies, San Fransisco, 2003.

[11] Synthesis Energy Systems. Plants -licensed SGT projects. http://www.synthesisenergy.com/plants, 2017.

[12] Xu, G., Murakami, T., Suda, T., Matsuzawa, Y., Tani, H. The superior technical choice for dual fluidized bed gasification. *Industrial and Engineering Chemistry Research*, 2006, 45, 2281-2286.

[13] Gunnarsson, I. The GoBiGas Project; Technical Report. Göteborg Energi, Göteborg, Sweden, 2011.

[14] Repotec. Biomass CHP Plant Senden. http://www.repotec.at/index.php/96.html, 2018.

[15] Fushimi, C., Wada, T., Tsutsumi, A. Inhibition of steam gasification of biomass char by hydrogen and tar. *Biomass and Bioenergy*, 2011, 35, 179-185.

[16] Bhatia, S.K., Perlmutter, D.D. A random pore model for fluid-solid reactions: I. Isothermal, kinetic control. *AlChE Journal*, 1980, 26, 379–386.

[17] Ishida, M., Wen, C.Y. Comparison of zone-reaction model and unreacted-core shrinking model in solid-gas reactions - I Isothermal analysis. *Chemical Engineering Science*, 1971, 26, 1031-1041.

[18] Ondrey, G. Startup for a new gasification process. *Chemical Engineering*, 2015, 122, 10.

[19] Barrio, M., Gøbel, B., Risnes, H., Henriksen, U., Hustad, J.E., Sørensen, L.H. Steam gasification of wood char and the effect of hydrogen inhibition on the chemical kinetics. In: Bridgwater, A.V. (Ed.), Progress in Thermochemical Biomass Conversion, Blackwell Science, U.K., 2001.

[20] Sette, E., Pallarès, D., Johnsson, F. Influence of bulk solids cross-flow on lateral mixing of fuel in dual fluidized beds. *Fuel Processing Technology*, 2015, 140, 245-251.

[21] Chirone, R., Miccio, F., Scala, F. On the relevance of axial and transversal fuel segregation during the FB combustion of a biomass. *Energy and Fuels*, 2004, 18, 1108-1117.

[22] Di Blasi, C. Combustion and gasification rates of lignocellulosic chars. *Progress in Energy and Combustion Science*, 2009, 35, 121-140.

[23] Gómez-Barea, A., Leckner, B. Modeling of biomass gasification in fluidized bed. *Progress in Energy and Combustion Science*, 2010, 36, 444-509.

[24] Nilsson, S., Gómez-Barea, A., Cano, D.F. Gasification reactivity of char from dried sewage sludge in a fluidized bed. *Fuel*, 2012, 92, 346-353.

[25] Winter, F. The Concept of Chemical Similarity for Optimization and Design of Gas-Solid Processes. Habilitation, Technisch-Naturwissenschaftliche Fakultät, Technical University of Vienna, Vienna, 1999.

[26] Liu, H., Zhu, H., Kaneko, M., Kato, S., Kojima, T. High-temperature gasification reactivity with steam of coal chars derived under various pyrolysis conditions in a fluidized bed. *Energy and Fuels*, 2010, 24, 68-75.

[27] Scott, S.A., Davidson, J.F., Dennis, J.S., Fennell, P.S., Hayhurst, A.N. The rate of gasification by CO2 of chars from waste. *Proceedings of the Combustion Institute*, 2005, 30, 2151-2159.

[28] Nilsson, S., Gómez-Barea, A., Fuentes-Cano, D., Campoy, M. Gasification kinetics of char from olive tree pruning in fluidized bed. *Fuel*, 2014, 125, 192-199.

[29] Kojima, T., Assavadakorn, P., Furusawa, T. Measurement and evaluation of gasification kinetics of sawdust char with steam in an experimental fluidized bed. *Fuel Processing Technology*, 1993, 36, 201-207.

[30] Qin, K., Thunman, H. Diversity of chemical composition and combustion reactivity of various biomass fuels. *Fuel*, 2015, 147, 161-169.

[31] Perander, M., DeMartini, N., Brink, A., Kramb, J., Karlström, O., Hemming, J., Moilanen, A., Konttinen, J., Hupa, M. Catalytic effect of Ca and K on CO2 gasification of spruce wood char. *Fuel*, 2015, 150, 464-472.

[32] Mitsuoka, K., Hayashi, S., Amano, H., Kayahara, K., Sasaoaka, E., Uddin, M.A. Gasification of woody biomass char with CO2: The catalytic effects of K and Ca species on char gasification reactivity. *Fuel Processing Technology*, 2011, 92, 26-31.

[33] Adschiri, T., Shiraha, T., Kojima, T., Furusawa, T. Prediction of CO2 gasification rate of char in fluidized bed gasifier. *Fuel*, 1986, 65, 1688-1693.

[34] Goring, G.E., Cursan, G.P., Tarbox, R. P., Gorin, E. Kinetics of Carbon Gasification by Steam. *Industrial and Engineering Chemistry*, 1952, 44, 1051-1065.

[35] Nilsson, S., Gómez-Barea, A., Ollero, P. Gasification of char from dried sewage sludge in fluidized bed: Reaction rate in mixtures of CO2 and H2O. *Fuel*, 2013, 105, 764-768.

[36] Cetin, E., Moghtaderi, B., Gupta, R., Wall, T.F. Influence of pyrolysis conditions on the structure and gasification reactivity of biomass chars. *Fuel*, 2004, 83, 2139-2150.

[37] Rocca, P.A.D., Cerrella, E.G., Bonelli, P.R., Cukierman, A.L. Pyrolysis of hardwoods residues: on kinetics and chars characterization. *Biomass and Bioenergy*, 1999, 16, 79-88.

[38] Kurosaki, F., Ishimaru, K., Hata, T., Bronsveld, P., Kobayashi, E., Imamura, Y. Microstructure of wood charcoal prepared by flash heating. *Carbon*, 2003, 41, 3057-3062.

[39] Chen, G., Yu, Q., Sjöström, K. Reactivity of char from pyrolysis of birch wood. *Journal of Analytical and Applied Pyrolysis*, 1997, 40–41, 491-499.

[40] Fushimi, C., Araki, K., Yamaguchi, Y., Tsutsumi, A. Effect of heating rate on steam gasification of biomass. 1. Reactivity of char. *Industrial and Engineering Chemistry Research*, 2003, 42, 3922-3928.

[41] Kumar, M., Gupta, R.C. Influence of carbonization conditions on the gasification of acacia and eucalyptus wood chars by carbon dioxide. *Fuel*, 1994, 73, 1922-1925.

[42] Mermoud, F., Salvador, S., Van de Steene, L., Golfier, F. Influence of the pyrolysis heating rate on the steam gasification rate of large wood char particles. *Fuel*, 2006, 85, 1473-1482.

[43] Tchoffor, P.A., Davidsson, K.O., Thunman, H. Transformation and release of potassium, chlorine, and sulfur from wheat straw under conditions relevant to dual fluidized bed gasification. *Energy and Fuels*, 2013, 27, 7510-7520.

[44] Sun, K., Jiang, J.c. Preparation and characterization of activated carbon from rubber-seed shell by physical activation with steam. *Biomass and Bioenergy*, 2010, 34, 539-544.

[45] Sette, E., Berdugo Vilches, T., Pallarès, D., Johnsson, F. Measuring fuel mixing under industrial fluidized-bed conditions - A camera-probe based fuel tracking system. *Applied Energy*, 2016, 163, 304-312.

[46] Arjmand, M., Leion, H., Lyngfelt, A., Mattisson, T. Use of manganese ore in chemical-looping combustion (CLC)-Effect on steam gasification. *International Journal of Greenhouse Gas Control*, 2012, 8, 56-60.

[47] Linderholm, C., Lyngfelt, A., Cuadrat, A., Jerndal, E. Chemical-looping combustion of solid fuels - Operation in a 10 kW unit with two fuels, above-bed and in-bed fuel feed and two oxygen carriers, manganese ore and ilmenite. *Fuel*, 2012, 102, 808-822.

[48] Berdugo Vilches, T., Marinkovic, J., Seemann, M., Thunman, H. Comparing Active Bed Materials in a Dual Fluidized Bed Biomass Gasifier: Olivine, Bauxite, Quartz-Sand, and Ilmenite. *Energy and Fuels*, 2016, 30, 4848-4857.

[49] Rapagnà, S., Jand, N., Kiennemann, A., Foscolo, P.U. Steam-gasification of biomass in a fluidised-bed of olivine particles. *Biomass and Bioenergy*, 2000, 19, 187-197.

[50] Tchoffor, P.A., Davidsson, K., Thunman, H. Effects of Steam on the Release of Potassium, Chlorine, and Sulfur during Char Conversion, Investigated under Dual-Fluidized-Bed Gasification Conditions. *Energy and Fuels*, 2014, 28 6953−6965.

[51] Keller, M., Leion, H., Mattisson, T. Mechanisms of Solid Fuel Conversion by Chemical-Looping Combustion (CLC) using Manganese Ore: Catalytic Gasification by Potassium Compounds. *Energy Technology*, 2013, 1, 273-282.

[52] Berdugo Vilches, T., Maric, J., Knutsson, P., Rosenfeld, D.C., Thunman, H., Seemann, M. Bed material as a catalyst for char gasification: The case of ash-coated olivine activated by K and S addition. *Fuel*, 2018, 224, 85-93.

[53] Kunii, D., Levenspiel, O. Fluidization Engineering. Butterworth-Heinemann, Newton, 1991.

[54] Svensson, A., Johnsson, F., Leckner, B. Fluidization regimes in non-slugging fluidized beds: the influence of pressure drop across the air distributor. *Powder Technology*, 1996, 86, 299-312.

[55] Pallarès, D. Fluidized bed combustion -modelling and mixing. Doctoral thesis, Energy and Environment, Chalmers University of Technology, Göteborg, Sweden, 2008.

[56] Hannes, J.P. Mathematical Modelling of Circulating Fluidized Bed Combustion. Doctoral thesis, Technical University of Delft, Delft, Netherlands, 1996.

[57] Ratschow, L. Three-Dimensional Simulation of Temperature Distributions in Large-Scale Circulating Fluidized Bed Combustors. Doctoral thesis, Technical University of Hamburg-Harburg, Hamburg, Germany, 2009.

[58] Myöhänen, K. Modelling of combustion and sorbent reactions in three-dimensional flow environment of a circulating fluidized bed furnace. Doctoral thesis, Lappeenranta University of Technology, Lappeenranta, Finland, 2011.

[59] Nikoo, M.B., Mahinpey, N. Simulation of biomass gasification in fluidized bed reactor using ASPEN PLUS. *Biomass and Bioenergy*, 2008, 32, 1245-1254.

[60] Jiang, H., Morey, R.V. A numerical model of a fluidized bed biomass gasifier. *Biomass and Bioenergy*, 1992, 3, 431-447.

[61] Radmanesh, R., Cnaouki, J., Guy, C. Biomass gasification in a bubbling fluidized bed reactor: Experiments and modeling. *AIChE Journal*, 2006, 52, 4258-4272.

[62] Petersen, I., Werther, J. Three-dimensional modeling of a circulating fluidized bed gasifier for sewage sludge. *Chemical Engineering Science*, 2005, 60, 4469-4484.

[63] Myöhänen, K., Palonen, J., Hyppänen, T. Modelling of indirect steam gasification in circulating fluidized bed reactors. *Fuel Processing Technology*, 2018, 171, 10-19.

[64] Sofialidis, D., Faltsi, O. Simulation of biomass gasification in fluidized beds using computational fluid dynamics approach. *Thermal Science*, 2001, 5, 95-105.

[65] Wang, Y., Yan, L. CFD modeling of a fluidized bed sewage sludge gasifier for syngas. *Asia-Pacific Journal of Chemical Engineering*, 2008, 3, 161-170.

[66] Gerber, S., Oevermann, M. A two dimensional Euler-Lagrangian model of wood gasification in a charcoal bed - Part I: Model description and base scenario. *Fuel*, 2014, 115, 385-400.

[67] Jennen, T., Hiller, R., Köneke, D., Weinspach, P.M. Modeling of gasification of wood in a circulating fluidized bed. *Chemical Engineering and Technology*, 1999, 22, 822-826.

[68] Israelsson, M., Berdugo Vilches, T., Thunman, H. Conversion of Condensable Hydrocarbons in a Dual Fluidized Bed Biomass Gasifier. *Energy and Fuels*, 2015, 29, 6465-6475.

[69] Berdugo Vilches, T., Seemann, M., Thunman, H. Influence of ash-coated olivine on tar formation in steam gasification of biomass. *To be submitted*, 2018.

[70] Sette, E., Pallarès, D., Johnsson, F. The influence of operating conditions and fuel-feed location on fuel residence time in an indirect gasifier. 11th International Conference on Fluidized Bed Technology, CFB 2014, Chemical Industry Press, Beijing, 2014, pp. 809-814.

[71] Lu, G.Q., . Do, D.D. Comparison of structural models for high-ash char gasification. *Carbon*, 1994, 32, 247-263.

[72] Lundberg, L., Pallarès, D., Johansson, R., Thunman, H. A 1-dimensional model of indirect biomass gasification in a dual fluidised bed system. 11th International Conference on Fluidized Bed Technology, CFB 2014, Chemical Industry Press, Beijing, 2014, pp. 607-612.

[73] Sette, E., Pallarès, D., Johnsson, F. Experimental quantification of lateral mixing of fuels in fluid-dynamically down-scaled bubbling fluidized beds. *Applied Energy*, 2014, 136, 671-681.

[74] Oka, S. Fluidized Bed Combustion. Marcek Dekker Inc, New York, 2004.

[75] Darton, R.C., LaNauze, R.D., Davidson, J.F., Harrison, D. Bubble growth due to coalescence in fluidised beds. *Trans Inst Chem Eng*, 1977, 55, 274-280.

[76] Wen, C.Y., Yu, Y.H. A generalized method for predicting the minimum fluidization velocity. *AIChE Journal*, 1966, 12, 610-612.

[77] Cui, H., Mostoufi, N., Chaouki, J. Characterization of dynamic gas–solid distribution in fluidized beds. *Chemical Engineering Journal*, 2000, 79, 133-143.

[78] Toomey, R.D., Johnstone, H.F. Gaseous fluidization of solid particles. *Chemical Engineering Progress*, 1952, 48, 220-225.

[79] Bruni, G., Solimene, R., Marzocchella, A., Salatino, P., Yates, J.G., Lettieri, P., Fiorentino, M. Self-segregation of high-volatile fuel particles during devolatilization in a fluidized bed reactor. *Powder Technology*, 2002, 128, 11-21.

[80] Lundberg, L., Tchoffor, P.A., Johansson, R., Pallarès, D. Determination of Kinetic Parameters for the Gasification of Biomass Char Using a Bubbling Fluidised Bed Reactor. 22nd International Conference on Fluidized Bed Conversion, Turku, Finland, 2015.

[81] Leva, M. Fluidization. McGraw-Hill, New York, 1959.

[82] Israelsson, M., Larsson, A., Thunman, H. Online measurement of elemental yields, oxygen transport, condensable compounds, and heating values in gasification systems. *Energy and Fuels*, 2014, 28, 5892-5901.

[83] Neves, D., Thunman, H., Matos, A., Tarelho, L., Gómez-Barea, A. Characterization and prediction of biomass pyrolysis products. *Progress in Energy and Combustion Science*, 2011, 37, 611-630.